FINAL TECHNICAL REPORT (FTR)

USING LANDSLIDE-DAMMED LAKES TO IDENTIFY COSEISMIC SLOPE INSTABILITY IN CASCADIA: COLLABORATIVE RESEARCH WITH UNIVERSITY OF OREGON AND UNIVERSITY OF TEXAS

Award Numbers: G18AP00011 & G18AP00012

Start and End Date: January 1, 2018 to December 31, 2018

by William T. Struble[1], Joshua J. Roering[1], Bryan A. Black[2], William J. Burns[3], Nancy Calhoun[3], Logan Wetherell[4]

[1]Department of Earth Sciences, 1272 University of Oregon, Eugene, Oregon 97403, USA

[2]Laboratory of Tree Ring Research, University of Arizona, 1215 E. Lowell Street, Tucson, Arizona 85721, USA

[3]Oregon Department of Geology and Mineral Industries, 800 NE Oregon Street, Portland, Oregon 97232, USA

[4]Dept of Geological Sciences, Central Washington University, 400 E. University Way, Ellensburg, Washington 98926, USA

ACKNOWLEDGEMENT OF SUPPORT AND DISCLAIMER

- This material is based upon work supported by the U.S. Geological Survey under Grant No. (G18AP00011 & G18AP00012).
- The views and conclusions contained in this document are those of the authors and should not be interpreted as representing the opinions or policies of the U.S. Geological Survey. Mention of trade names or commercial products does not constitute their endorsement by the U.S. Geological Survey.

ABSTRACT

Large magnitude earthquakes and climatic events in mountainous settings commonly trigger thousands of landslides, and these slope failures typically constitute a significant proportion of the damage associated with these events. Large, dormant deep-seated landslides are ubiquitous in the Oregon Coast Range (OCR), USA, yet a method for calculating landslide ages with accuracy required to diagnose a specific triggering event, including the 1700 AD Cascadia earthquake, has remained elusive. Establishing a compelling connection between pre-historic slope instability and specific triggers requires landslides ages with accuracy greater than that provided by ^{14}C dating of detrital materials. Tree ring analysis is the only known method capable of determining landslide age with this accuracy. Dozens of landslide-dammed lakes in western Oregon present an opportunity to use tree rings from drowned snags, or 'ghost forests,' to establish the year of death, and thus landsliding. We crossdate tree ring indices from drowned Douglas-fir trees with existing live tree ring records from the OCR that exhibit synchronous, time-specific patterns due to regional climate variations. Our analyses determine that the landslides responsible for creating Wasson and Klickitat Lakes occurred in 1819 and 1751 AD, respectively. ^{14}C dates from selected tree rings and landslide deposit detritus are consistent with our tree ring analysis, although the ages exhibit high variability, revealing the limitations of using ^{14}C dating alone. Because dendrochronology provides annual accuracy of landsliding, sampling tree rings at additional landslide-dammed lakes throughout the OCR can be used to constrain the potential effects of ground motion and major climatic events on Cascadia landscapes.

REPORT

INTRODUCTION

Despite improved resolution of the recurrence interval of large magnitude subduction zone earthquakes in Cascadia (Goldfinger et al., 2012), prediction of ground motion and landscape response remains highly uncertain (Allstadt et al., 2013). The Cascadia subduction zone has produced numerous

large (>M 9.0) earthquakes, with an average recurrence interval of 300-500 years (Goldfinger et al., 2012). The timing of the most recent earthquake, which occurred on the evening of January 26, 1700, was constrained in part by a combination of offshore turbidite records (Goldfinger et al., 2012); the dendrochronology of 'ghost forests' that were drowned by coseismic subsidence and the resultant tsunami (Atwater and Yamaguchi, 1991; Yamaguchi et al., 1997); and the arrival of the tsunami in Japan (Atwater et al., 2005). During future subduction zone earthquakes, the magnitude of shaking is locally uncertain (Allstadt et al., 2013), although shaking is expected to be high along the coast, with peak ground acceleration (PGA) values 0f 0.4 g (percent of gravity) and higher. Shaking will attenuate inland towards the Willamette Valley and the Cascades, though PGA will remain high throughout the Oregon Coast Range, in excess of 0.2 g (Figure 1; Madin and Burns, 2013; Olsen et al., 2015). High intensity and long duration shaking may affect landslide reactivation differently than expected for shallow, crustal earthquakes (Meunier et al., 2008, 2007).

Historically, earthquakes produce 10^4 to 10^5 landslides (Keefer, 2002, 1984). In many landscapes, a significant proportion of total erosion occurs due to coseismic landslides (Dadson et al., 2004; Densmore and Hovius, 2000; Hovius et al., 2011; Li et al., 2014; Marc et al., 2016a), the distribution of which is often spatially variable and complicated. In many cases, the spatial density of earthquake-induced landsliding varies systematically with ground motion (Meunier et al., 2007), whereas distance to fault rupture provides a more robust relationship for other seismic events (Massey et al., 2018). Over 15,000 landslides were triggered in the 2008 Wenchuan earthquake (Li et al., 2014), and in the 2015 Gorkha, Nepal earthquake, landslides increased in density over 100 km away from the epicenter (Roback et al., 2017). In addition, low rock strength often determines the pattern of coseismic slope instability (Newmark, 1965), as made apparent in the 2011 Tohoku earthquake where >80 percent of the >3,400 landslides occurred in Quaternary sediments and weak Neogene rock units (Wartman et al., 2013).

Probabilistic models are useful for predicting where landsliding will be most pervasive during earthquakes and the volume of coseismic landslides (Jibson et al., 2000; Keefer, 1984). Keefer (1984) noted a power law scaling relationship between seismic moment and total landslide volume. The volume of landslides associated with subduction zone earthquakes, however, is often significantly less than that predicted by the power law scaling relationship (Marc et al., 2016b), although the number of subduction zone earthquake inventories is very limited (Tanyaş et al., 2017, 2018). By contrast, at least one subduction zone earthquake deviates markedly from this trend. The 1960 Chilean earthquake caused approximately 250 square kilometers of the proximal terrain to experience landsliding (Veblen and Ashton, 1978), which when applied to the area-volume relationship of Larsen et al. (2010), produces a resultant landslide volume much larger than subduction zone earthquakes of a similar magnitude. Hence, the apparent paucity of landslides during some subduction zone earthquakes may partially be accounted for by the limited number of subduction zone earthquakes that have been addressed with landslide inventories relative to shallow crustal earthquakes (Marc et al., 2016b). If the recent datasets are representative, the low rates of landslides during subduction zone events may additionally be due to seismic attenuation, great depth of the hypocenter, and the directivity of seismic waves away from shore (Gallen et al., 2016; Gorum et al., 2014; Kargel et al., 2016; Meunier et al., 2008, 2007). Regardless, the observed variability in slope failure during subduction zone earthquakes warrants investigation of past slope failures in Cascadia.

The coastal and forearc regions of Cascadia exhibit a long history of widespread slope instability (Roering et al., 2005; Schulz et al., 2012). In the OCR, the geologic and topographic signature of

landsliding is pervasive; steep topography and weak lithologic units combine to promote slope instability over a range of timescales (Burns et al., 2012; Roering et al., 2005; Schmidt and Montgomery, 1995). Here, thousands of shallow, colluvial landslides and debris flows associated with intense rainfall have been historically observed (Montgomery et al., 2000; Robison et al., 1999). However, all of the >40,000 known deep-seated landslides (Burns and Watzig, 2014) appear to have formed prior to European settlement, which suggests that the conditions promoting pervasive deep-seated instability have not been realized in recent decades or longer. Elsewhere, deep-seated landslides are common during large magnitude earthquakes, particularly in areas of high relief (e.g., Gallen et al., 2016; Kargel et al., 2016; Keefer, 1984; Marc et al., 2016; Roback et al., 2017; Valagussa et al., 2019). Yet, no subaerial landslide in Cascadia has been definitively linked to a subduction zone earthquake, including the January 26, 1700 AD earthquake (Atwater et al., 2005; Goldfinger et al., 2012; Karlin et al., 2004; Leithold et al., 2018; Schulz et al., 2012; Schuster et al., 1992). Here, we use dendrochronological methods to date two landslides in the OCR with sub-annual accuracy with particular interest in links to the 1700 AD subduction zone earthquake. However, as this approach is more broadly applied, it holds the potential to identify synchrony among landslide events and infer mechanisms of slope failure, whether from earthquake-induced ground motion or extreme climatic events.

Dating pre-Historic Landslides

Landslides have been dated using surface exposure dating and the dendrochronology of live trees on deposits (Ballantyne and Stone, 2004; Fantucci and McCord, 1995; Ivy-Ochs et al., 2009; Lang et al., 1999; Stefanini, 2004; and many others), although, radiocarbon (^{14}C) dating is the most common method (Benda, 1990; Booth et al., 2017; Clague, 2015; Lang et al., 1999; Reneau et al., 1986; Reneau and Dietrich, 1991; and many others). ^{14}C dating of detrital materials in sediments is particularly applicable in the OCR due to the abundance of datable organic material (e.g. Benda, 1990; Reneau et al., 1986; Reneau and Dietrich, 1991) and has been used elsewhere to build comprehensive landslide chronologies and calibrate other relative dating techniques. For example, surface roughness-age calculations of landslides have been calibrated by ^{14}C dating (e.g. Booth et al., 2017; LaHusen et al., 2016; McKean and Roering, 2004) as have tephrochronologies that inform volcanic eruptive histories (Braitseva et al., 1993) and reconstructions of paleolandscapes (Cerovski-Darriau et al., 2014; Danišík et al., 2012).

While these techniques have provided useful datasets of landslide recurrence in various landscapes, their accuracy is not adequate to date recent landslides or tie them to specific triggering events. Surface exposure dating is limited when field relationships between sampled surfaces are not clear (Ballantyne and Stone, 2004; Ivy-Ochs et al., 2009), and landslides must be sufficiently large to expose fresh and shielded bedrock (Lang et al., 1999). Radiocarbon dating has inherent uncertainty due to varying production rates of ^{14}C in the atmosphere, made evident in the 'wiggles' of the radiocarbon calibration curve. Some portions of this curve oscillate more than others, which complicates dating of landslides that occurred during these episodes (Figure 8; Reimer et al., 2009). Further complicating accuracy, ^{14}C dating usually neglects the residence time of detrital material, which may remain on the landscape undisturbed for millennia prior to landslide emplacement (Clague, 2015; Gavin, 2003, 2001; Trumbore, 2000). ^{14}C dating additionally does not consider reactivation of deep-seated landslides; a ^{14}C date for a reactivated landslide may provide the age of the initial failure, not the most recent. Finally, ^{14}C dating often relies on dating charcoal, which is subject to high uncertainty due to high post-fire residence times (Gavin, 2003, 2001; Reneau et al., 1986; Reneau and Dietrich, 1991; Trumbore, 2000).

Ultimately, ^{14}C dating cannot provide the annual accuracy necessary to connect landslide failures to a specific event, or to identify clustering of landslides associated with a particular triggering event.

STUDY AREA

Oregon Coast Range

The Oregon Coast Range (OCR) is a steep and dissected mountain range subject to uplift along the Cascadia subduction zone. The OCR has a Mediterranean climate with cool, wet winters when the majority of the annual 1-2 m of precipitation falls, and dry, warm summers (PRISM Climate Group, 2016). The hillslopes are soil-mantled and support tree populations of Douglas-fir (*Pseudotsuga menziesii*) and western Hemlock (*Tsuga heterophylla*). The dominant lithology in the OCR is a ~3 km thick interbedded turbidite sequence of Eocene sandstones and siltstones known as the Tyee Formation, which rest on accreted volcanic terranes (Heller and Dickinson, 1985; Wells et al., 1998). Previous work has generally placed the provenance of the sediments within the Tyee Formation as either the Idaho Batholith or the Klamath Mountains (Dumitru et al., 2013; Heller et al., 1985; Heller and Dickinson, 1985). Since deposition in the Eocene and subsequent uplift in the Miocene, the Tyee Formation has experienced 40º to 70º of clockwise rotation at 1º/m.y., primarily due to oblique subduction and extension in the Basin and Range Province and northward migration of the Sierra Nevada block (Heller and Ryberg, 1983; McNeill et al., 2000; Wells et al., 1998; Wells and Heller, 1988; Wells and McCaffrey, 2013). This rotation has resulted in the deeper marine facies of the Tyee Formation, and hence a higher proportion of siltstone to sandstone, in the northern portion of the OCR, with a higher proportion of sandstone remaining in the south (Roering et al., 2005). This rotation also places the OCR in a compressive regime, resulting in minor deformation and folding, with dips along fold limbs typically less than 15º-20º (Baldwin, 1956).

On the steep ridge-valley terrain in the OCR, soils are produced from bedrock primarily through tree throw and are thinnest (~0.5 m) on the ridges and adjacent hillslopes (Dietrich and Dunne, 1978). Soils thicken (~1-2 m) in the unchanneled valleys, which are periodically evacuated by shallow landslides that often mobilize into debris flows (Benda and Dunne, 1997; Dietrich and Dunne, 1978; Stock and Dietrich, 2003). The OCR has often been described as an example of a steady state landscape, where uplift is balanced by erosion (Montgomery, 2001; Reneau and Dietrich, 1991). Studies of cosmogenic erosion rates have shown that the OCR is eroding approximately 0.05 – 0.14 mm yr^{-1} (Balco et al., 2013; Heimsath et al., 2001; Penserini et al., 2017), while marine terraces along the coast further suggest uplift rates of 0.05 – 0.3 mm yr^{-1} (Kelsey et al., 1996, 1994; Kelsey and Bockheim, 1994), with strath terraces suggesting similar rates of 0.1 – 0.2 mm yr^{-1} (Personius, 1995). How far inland these uplift rates extend is generally poorly constrained, although Penserini et al. (2017) found morphologic evidence that erosion and uplift rates, assuming steady erosion, experience a modest increase in the eastward (inland) direction.

Deep-seated landslides are most common on dip slopes of sandstone-siltstone turbidite interbeds of the Tyee Formation (Roering et al., 2005). The density of deep-seated sliding varies with latitude reflecting the dominance of sandstone and siltstone interbeds such that the southern portion of the range, where sandstone is the more common component of the Tyee Formation, exhibits fewer large landslides (Burns et al., 2012; Roering et al., 2005). Because the spatial distribution of landslides correlates strongly with lithology and geologic structure rather than the inland attenuation of ground motion from subduction zone earthquakes (Madin and Burn, 2013; Olsen et al., 2015), the application of coseismic landslide model predictions is complex, especially given the broad range of landslide triggering mechanisms (Allstadt et al., 2013).

The paucity of historic deep-seated landslide activity and the potentially broad range of landslide ages complicates efforts to link landslides with specific seismic or climatic events. Specifically, despite the existence of >40,000 deep-seated landslides in the OCR (Burns and Watzig, 2014), few to none have been observed to fail catastrophically or form landslide dams, with the notable exception being the Drift Creek landslide reactivation in 1975 that followed heavy and prolonged rain (Thrall et al., 1980). Meanwhile, the landslide responsible for the formation of Triangle Lake occurred ~50 ka (Marshall et al., 2017), and soil residence times suggest some of the largest deep-seated landslides are on the order of 100 ka or older (Almond et al., 2007). Such an extensive history of landsliding may reflect numerous individual triggering events (or episodes of activity) for each landslide. More importantly, however, the tendency for landslides to experience reactivation enables us to test whether earthquakes and storms act as potential triggers.

Landslide-dammed Lakes

A causal relation between slope failure and triggering events such as subduction zone earthquakes or large storms requires the acquisition of landslide ages with accuracy greater than that provided by ^{14}C dating of detrital materials, which typically has >10-yr standard error. Dendrochronology is the only known method with the potential to estimate landslide age with annual (or potentially sub-annual) accuracy. There exist dozens of landslide-dammed lakes in western Oregon with standing Douglas-fir snags, or 'ghost forests' (Figure 1). Standing dead trees at landslide-dammed lakes are, by themselves, unremarkable; their location and current submerged state, however, renders their history intriguing. Tree rings from these standing Douglas-fir snags can be analyzed to date the year of death of the trees, reminiscent of the paleoseismic work of Yamaguchi et al. (1997), who used drowned trees on the coast of Cascadia to constrain the timing of the January 26, 1700 AD earthquake. These 'ghost forests' died when large landslides clogged proximal valley bottoms, damming stream channels. Rapid valley inundation followed landslide dam emplacement, resulting in the death of the submerged trees. Landslide dam emplacement also initiated alluviation upstream of the dam, which is additionally useful for estimating time since landslide emplacement. In the OCR, lidar analysis reveals a multitude of such landslide-dammed lakes, with deposit morphology suggesting triggering within the last several hundred years (Figures 2, 3). These landslide-dammed lakes afford a unique opportunity to determine whether the timing of the landslides corresponds with major Cascadia earthquakes.

METHODS

Site Selection and Mapping

Using high-resolution airborne lidar-derived bare earth digital elevation models (DEMs; DOGAMI, 2012, 2015), we located >200 sites with topographic evidence of landslide-dammed lakes throughout the OCR. These sites were investigated further to clarify those that appear young enough to be potentially associated with the 1700 AD earthquake (Atwater et al., 2005). We selected landslide-dammed lake sites that display characteristics that are consistent with relatively recent (hundreds of years) landslide movement, in particular fresh morphologic features such as sharp headscarps and minimal channel incision of the deposit (Booth et al., 2017, 2009; Burns and Madin, 2009; LaHusen et al., 2016). We examined each potential landslide dam for the presence of an existing lake or marsh upstream of the deposit, and we used aerial imagery (USDA, 2000) to ascertain the existence of standing snags. Lakes were prioritized according to land ownership and accessibility to trees, the presence of delta progradation and marginal sedimentation aiding in access.

Once the sites were selected for field reconnaissance, we completed detailed mapping of the landslide features, current and estimated high-lake extent, and alluvium retained upstream of the

landslide dam (Figure 4). Initial field data and sample acquisition included: confirming the presence of landslide-dam, standing water, alluvium, and standing snags; verifying the survival of bark to confirm existence of outer growth increment and noting accessibility of standing snags for future sampling; and sampling standing snags' outer rings, detrital organics from within the landslide deposit for ^{14}C analysis, and increment cores from old-growth living trees on the landslide surface.

Snag Sampling and Measurement

We collected samples from dead Douglas-fir trees at two sites in the OCR, specifically Klickitat Lake (44.480, -123.659) and Wasson Lake (43.748, -123.795). Where Douglas-fir snags were readily accessible from shore, we excavated the base of each tree to expose fresh bark, sampling just below waterline for high preservation potential. Bark attached to the last growth increment is crucial for determining an accurate year (and potentially season) of death, as the interface between the bark and outermost growth ring demarcates the termination of the growth record. A lack of bark does not preclude dating of the landslide, though the calculated age must be considered a maximum age. A licensed sawyer extracted slabs or wedges at each tree; each slab ideally included >100 rings with bark at the outer edge and was sufficiently wide (>20 cm) relative to tree diameter to account for any variability in ring width around the tree. Care was taken to avoid sampling portions of trees with abnormal growth patterns potentially from fire damage or limb growth. We reburied any excavated portions of the trees to reduce visual impact. Slabs were promptly dried to reduce mold growth and preserve the possibility of radiocarbon dating.

We used the dendrochronology technique of crossdating to establish the calendar year of death from drowned snags, and thus the age of the landslide damming event. As trees grow, limiting factors such as drought result in synchronous, time-specific growth patterns among individuals of a given species and region (Bekker et al., 2018; Douglass, 1941; Yamaguchi et al., 1997). Black et al. (2015) generated three >400 yr Douglas-fir chronologies for the OCR and four >800 yr chronologies in the western Cascade Range that reveal strong regional correlation (Figure 1). We crossdated the ring measurements from 'ghost forest' trees at landslide-dammed lakes against both locations to determine the timing of death, which corresponds to the calendar year of the last growth increment. We were often able to estimate the season of death by the extent to which the final increment formed; termination of growth during formation of dark, late wood suggests death in the late summer to winter, while the partial development of light, early wood implies a death in late winter to spring.

After collecting and drying each slab, we sanded the slab surfaces progressively finer, finishing at 400 grit and adding a final polish with 12-micron lapping film. Samples within a given site were visually crossdated using the list-year technique (Yamaguchi, 1991). Next, we used high-resolution scans (>2400 dpi) of slab surfaces to measure rings with the dendrochronology software, CooRecorder (Larsson, 2013). Each slab was measured twice along different transects to account for any growth irregularities around the circumference of the tree. Using the tree ring software, CDendro (Larsson, 2013), high-frequency, year-to-year variability was isolated within each measurement time series. These high-frequency patterns, which meet the statistical assumption of serial independence, were first compared among measurement time series within each site. Correlation coefficients were generated as were "T-tests" that compensate for differences in the number of overlapping years, calculated as

$$T\ value = c\sqrt{\frac{n-2}{1-c^2}}, \qquad (2)$$

where c is the correlation coefficient and n is the number of overlapping years (Larsson, 2013). Correlation and T-tests were lagged forwards and backwards over as many years as possible while maintaining a minimum of 30 years of overlap. Correct dating was established if the correlation coefficient was highly significant ($p < 0.01$), and it, along with the T-test value, were conspicuously greater than that of any other lag.

Measurement time series could be dated relative to one another within each site, but that did not provide information regarding the calendar years over which the trees lived. To generate dates tied to calendar year, the high-frequency variability from each measurement timeseries (that had been dated relative to one another) was averaged within the site. This floating mean chronology was then compared to the high-frequency variability from living trees at Marys Peak in the OCR (Black et al., 2015) using lagged correlations and T-test values. A lake was considered dated if there was a conspicuously prominent, highly significant ($p < 0.01$) correlation coefficient and T-test value between the dead 'ghost forest' chronology and the chronology generated from live-collected trees (Figures 5, 6, and 7). An exact year of tree death could be established if the wood immediately under the bark was well preserved, and confidence in the date of the landslide event was increased if multiple trees at a site died in the same year.

Live Tree Coring

Some of the landslide deposits at landslide-dammed lakes in the OCR host live old-growth Douglas-fir trees. These trees denote the minimum age of the landslide, as old growth stands are unlikely to survive large, deep-seated landslide failures (Clague, 2015). Live old growth is particularly useful at some landslide-dammed lakes where drowned snags are poorly preserved and have no visible bark to demarcate the outer growth ring. No statistical correlation with existing tree ring chronologies is required with this method, as the age of the trees simply provides the minimum age of the landslide. The ecesis interval, or time between landslide occurrence and tree establishment, separates the age of the trees and the timing of the landslide and can span from a couple years to a century depending on the landscape (Clague, 2015). We used increment borers to collect 18 cores from 10 live Douglas-fir at Klickitat Lake and 4 cores from 4 western Hemlock at Wasson Lake to compare to the dendrochronology-derived age of the standing snags (Figures 9, 10). While this method is limited by the availability of old growth stands, which currently exist as a minor component of the harvest patchwork in the OCR, it remains a useful tool when used in concert with dendrochronology and radiocarbon dating.

^{14}C Dating: Tree Rings

We collected wood samples from slabs extracted from standing snags for ^{14}C analysis in order to corroborate the age of the landslide derived from dendrochronological techniques (Pringle, 2014; Schuster et al., 1992). As a tree grows, each progressive growth ring consumes and stores the relative concentration of ^{14}C present in the atmosphere. As such, tree rings record annual variations in atmospheric isotopic composition and can serve as a means to tune the radiocarbon calibration curve (Reimer et al., 2013). Because each ring precisely denotes a single year of growth in the tree, derived radiocarbon ages can be constrained by the calendar year of growth of each ring, a process known as 'wiggle matching' (Reimer et al., 2009). This process is particularly useful for improved ^{14}C dating of materials that are relatively young (<500 yr), as the radiocarbon calibration curve oscillates significantly throughout this time period (Figure 8).

We collected three wood samples from a slab from Wasson Lake, and two samples from a buried log in the landslide deposit at Klickitat Lake, for ^{14}C analysis. Each of the slabs from Wasson Lake

internally crossdate, so we are confident that collecting wood samples from only one tree is representative of the other slabs. For the Wasson Lake slab, we sampled wood from the outermost ring and rings 99 and 180 counted from the outside edge, rings sufficiently separated to effectively utilize Bayesian statistical methods. We used OxCal, a Bayesian statistical tool, to convert ^{14}C years to calendar years and constrain the age using wiggle matching (Ramsey, 1995). Wiggle matching utilizes the sequential order of the rings to constrain the calendar year probability distribution function (PDF) for each sample (Ramsey, 1995, 2009). For example, if the PDFs of rings 99 and 180 overlap, OxCal constrains the range of possible ages by recognizing that ring 99 is known to be exactly 81 years older than ring 180, thus shrinking the range of possible calendar year ages. We followed a similar approach for the buried log at Klickitat Lake. We collected the outermost preserved ring and wood from a ring approximately 52 rings inward. Given the decayed state of the wood, it was unclear how many rings may be missing from the outer edge of the tree, so the wiggle-matching derived age must be considered a maximum age of the landslide deposit. The ^{14}C ages from standing snags at Wasson Lake and the buried log at Klickitat Lake are also useful for interpreting the ages of the multitude of landslides in the OCR that lack dams and for which only deposits can be identified.

^{14}C Dating: Landslide Deposit Detritus

To test for radiocarbon inheritance and constrain how residence time of variable detritus-types biases calculated landslide ages, we preferentially selected small organic debris including charcoal, wood, and twigs. Traditional methods for dating landslides require collecting organic material from the landslide deposit, which is then dated using ^{14}C dating. We followed this approach at Klickitat and Wasson Lakes, and collected five pieces of detrital carbon from each deposit for dating. Where large pieces of wood or stumps were found, we sampled the outermost rings in order to derive the youngest and most accurate date possible. The various materials we sampled, including pieces of wood, twigs, leaves, and charcoal, were intended to constrain and demonstrate the types of materials that are considered preferable for dating landslides. Alternative materials such as wood or charcoal bias the calculated age relative to the dendrochronologically-derived date, which should be the most contemporaneous with landslide occurrence.

Sedimentation Rate Age

To estimate the number of years required to retain the volume of sediment ehind the landslide dams, we utilized the existing lidar-derived, bare earth, 1-meter DEMs and existing data on erosion rates for the OCR (Butterfield et al., 2015). Many previous studies have investigated the magnitude of erosion in the OCR, finding erosion rate values from cosmogenic nuclides spanning a range from 0.05 mm yr^{-1} to 0.2 mm yr^{-1} (Bierman et al., 2001; Heimsath et al., 2001 Marshall et al., 2015; Penserini et al., 2017; Reneau and Dietrich, 1991); Brown and Krygier (1971) and Beschta (1978) measured sediment yield rates between 0.05 and 0.08 mm yr^{-1}. Hence, based on these previously published erosion rates, we selected a range of erosion rate values from 0.05 to 0.2 mm yr^{-1} to use in our analysis.

We used the following equation:

$$T = \frac{V}{A \cdot E}, \qquad (1)$$

at Wasson and Klickitat Lakes, to calculate the time, T, required for deposition of the observed sediment volume, V, given the upstream drainage area, A, and erosion rate, E. We calculated the drainage area above the landslide dam using 1-meter DEMs in ArcMap. In order to calculate the sediment volume that has been deposited in the lakes since landslide emplacement, we estimated the pre-sediment infill topography. We drew surface elevation drainage and cross-section profiles above

and below the alluvium extent, which we used to estimate the pre-landslide drainage centerline elevation. We assumed all valleys to be v-shaped prior to sediment infilling. While we observe that the valley bottoms are not v-shaped, catchment area at both Klickitat and Wasson Lake is small enough that any variability in valley width is minor and will not greatly affect our calculations (May et al., 2013). The outer edge of the alluvium elevation was extracted as points from the current surface DEM, which were then combined and interpreted as a pre-landslide dam DEM. We subtracted this pre-landslide dam DEM from the modern DEM (Figure 4), which resulted in the total depth of lake water and sediment. We estimated an average lake depth from field observations, which along with lake surface area provided a total lake volume. We removed the lake volume from the total volume of the lake and sediment to yield the total sediment volume.

RESULTS

Klickitat Lake

We measured the rings from seven slabs and crossdated the slabs against each other to ensure that the trees at Klickitat Lake lived contemporaneously. After comparing the mean, undated Klickitat chronology against the Marys Peak chronology (Black et al., 2015), we determined the year of death to be in the winter of 1751/52 AD. The correlation coefficient for the floating chronology at Klickitat Lake and the Douglas-fir chronology from Marys Peak was 0.51 with a T-value of 8.1, values which are conspicuously high relative to other lagged dates (Figure 6). Using the cores that we collected from live trees on the surface of the landslide, we observed that the oldest trees began growing between 1760 and 1770 AD, approximately a decade after the landslide occurred (Figure 9). We are confident that the trees measured here accurately reflect the age of the landslide, as the trees on the landslide surface cannot be older than the lake.

To analyze the impact of radiocarbon inheritance on organic material in landslides, we collected and analyzed organic detrital material found within the landslide deposit including charcoal and woody debris ranging from twigs to pieces of entire trees. We found that collected detrital material at Klickitat Lake provides a wide range of ages. Specifically, two detrital charcoal samples provide ages of approximately 4400 – 4200 BC and 800 – 1000 AD, while woody material provides an age spanning from the early 1600s AD to near-present. We also collected two samples from two tree rings approximately 52 rings apart in a log buried in the landslide deposit, and using wiggle matching, these samples suggest a maximum landslide occurrence during the mid- to late-1600s AD (Figure 9). Thus, detrital carbon from the landslide deposit suggests a landslide age with high uncertainty, spanning over 6,000 years.

Using the sediment accumulation analysis above the dam, we determined an age range spanning from 82 to 330 years BP. The range of potential ages results from applying multiple sediment accumulation rates. Thus, the time required for the estimated volume of sediment to accumulate behind the landslide dam translates to landslide dam emplacement between 1688 and 1936 AD, which brackets our calculated dendrochronology age of 1751 AD.

Wasson Lake

We utilized multiple techniques to accurately constrain the age of the slide that created Wasson Lake. Following the same technique as Klickitat Lake, we measured and crossdated tree rings from three slabs at Wasson Lake and found the year of death for the trees to be the winter of 1819/20 AD. The correlation coefficient for the floating chronology from three samples at Wasson Lake and the Douglas-fir chronology from Marys Peak was 0.38 corresponding to a T-value of 6.0, values that are highly statistically significant ($p < 0.01$) and conspicuously greater than all other correlations (Figure 7).

Similar to Klickitat Lake, we are confident that rapid valley inundation following landslide emplacement killed the trees prior to further growth increments being added. We also observe from increment cores that live, old-growth western hemlock on the landslide surface began growing in the mid-1840s to early 1850s, a similar ecesis interval to that observed at Klickitat Lake.

In addition to dendrochronological analysis of slabs and minimum ages derived from live trees at Wasson Lake, we sampled three rings for radiocarbon analysis. We collected samples from a single slab and are confident that the ages derived from one tree will closely match the others, as they internally crossdate. The outermost ring yielded a modern ^{14}C age, which was not unexpected since the outer rings of all the slabs have undergone chemical alteration, made most apparent by discoloration in the outer ~5 cm of wood. Rings 99 and 180, however, yield ages of 105 ± 30 ^{14}C years and 235 ± 30 ^{14}C years, respectively. These ^{14}C ages correspond to two possible calendar year ages because each ^{14}C age crosses the radiocarbon calibration curve at multiple points. One scenario places the age of the dead tree between 1920 and 1990 AD (Figure 10). However, the time of landslide occurrence at Wasson Lake is not historically documented, and the trees on the landslide began growing in the 1840s AD, much too early for landslide occurrence to be in the twentieth century. The second scenario, spanning from 1810 to 1850 AD, is consistent with the year of death of 1819 AD derived from dendrochronology methods as well as the trees on the landslide deposit that began growing in the 1840s to early 1850s (Figure 10). Hence, despite higher uncertainty in these ages relative to the dendrochronology ages, these two radiocarbon samples from drowned snags help corroborate the landslide age.

In addition to collecting radiocarbon samples from rings of standing snags, we also collected detrital samples from the Wasson Lake landslide deposit. Two detrital charcoal samples date to approximately 7100 – 6700 BC and 1900 – 1700 BC. Two additional pieces of wood from the deposit date to approximately the late-1400s to mid-1600s AD and the mid-1600s AD to the near-present, respectively (Figure 10). Bark from a standing snag in Wasson Lake also had an age ranging from the early-1400s to early-1600s AD. In all, these ^{14}C dates alone would suggest a range of potential landslide ages spanning potentially over 9,000 years.

Similar to Klickitat Lake, we estimated the age of Wasson Lake based on sediment accumulation since landslide emplacement. Using several potential sedimentation rates, we determined a range of 138 to 553 years BP necessary to deposit the calculated total volume of sediment behind the landslide dam, which translates to landslide emplacement between 1465 and 1880 AD, bracketing our calculated age of 1819 AD.

Additional Landslide-dammed Lakes

We generated preliminary dates for several additional lakes using a combination of dendrochronology and radiocarbon. Calculated ages of landslides in the OCR generally do not correlate with known triggering events, including earthquakes and storms. An emerging number of sites, however, do demonstrate some temporal clustering. For example, Burchard and Esmond Lakes both date to the winter or early spring of 1890 AD. At both sites, the final correlated growth increments correspond to 1889 AD; however, trees at both sites have clearly discernable early wood, suggesting that the tree was still alive in the beginning of 1890 AD and died sometime in mid- to late-winter, or perhaps early spring. An age of 1890 AD at Burchard Lake is further corroborated by a wiggle matched tree branch found within the landslide deposit. We sampled wood from two rings separated by 80 rings. The outer sampled ring was approximately 99 rings from the outer edge of the wood. 14C ages for the branch include 245 ± 35 14C years for the inner sampled ring and 115 ± 30 14C years for

the outer sampled ring. When wiggle matched, this places the inner ring forming sometime between 1680 and 1730 AD and the outer ring growing between 1765 and 1810 AD. Counting 99 rings outward places tree death between 1864 and 1909 AD, bracketing the dendrochronology derived date of 1890 AD. Additional sites in the OCR do not exhibit similar temporal clustering, though the preliminary maximum ages at some sites do not preclude the possibility of clustering.

Site	Age	Number of Trees Correlated	Intercorrelation between trees? (Correlation coefficient)
Beaver Dam	Max 1926 AD	2	Yes (0.582)
Burchard	Winter 1889/1890 AD	3	Yes (0.468)
Carlton (small slide *into* lake)	Max 1785 AD	3	Yes (0.496)
Esmond	Winter 1889/1890 AD	3	Yes (0.528)
Ham	Max 1761 AD	2	Yes, moderate (0.369)
Hannah Creek	Max 1924 AD	3	Yes (0.369)
Hemlock	Indeterminate		No (rot, different species?)
Kaupi	Max 1869 AD	4	Yes (0.611)
Lobster	Max 1747 AD	2	Yes (0.721)
Murphy Grade Road	Max 1848 AD	3	Yes (0.713)
Parsons Creek	Max 1853 AD	4	Yes, moderate (0.419)
Pearl	Indeterminate		No, weak
Soup	Indeterminate (too old?)	3	Yes (0.518)
Spruce Run	Indeterminate		No
Sun	Indeterminate		No
Scoggins Valley	Max 1875 AD	1	No
Yellow	Indeterminate (too old?)	3	Yes (0.576)

DISCUSSION

Using dendrochronology of drowned trees to date landslides in Cascadia with high accuracy is novel, as it provides the only means to improve our ability to constrain the effects of past ground motion and high-magnitude precipitation events on Cascadian landscapes (Pringle, 2014; Weaver and Pringle, 2003). We are confident that the time of death we calculated for the ghost forests represents the age of the landslides; valley inundation will rapidly follow landslide emplacement, as recently observed for landslides triggered during the 2016 Kaikoura earthquake (Jibson et al., 2018). In addition, submergence of Douglas-fir roots should quickly result in tree mortality within a matter of weeks to a couple months (Gadgil, 1971), ending ring growth and preserving the ring sequence that we use here. While none of the landslides we date here are contemporaneous with the 1700 AD Cascadia subduction zone earthquake, it may be possible that the earthquake initially destabilized or conditioned slopes in the OCR, including at Klickitat and Wasson Lakes, with catastrophic failure occurring later (Schulz et al., 2012), a possibility that cannot currently be confirmed. Despite the lack of convincing contemporaneity with the 1700 AD event, the landslides we have dated extend existing western Oregon tree ring chronologies and may improve understanding of the climate-driven impacts on slope stability in the OCR. Furthermore, given the considerable number of deep-seated landslides in the OCR that remain undated – many of which impound lakes or marshes with standing snags – our approach presented here provides the opportunity to develop an unprecedented landslide database in Cascadia and beyond.

Advantages and Pitfalls of Radiocarbon

We utilized radiocarbon techniques to corroborate the ages of Klickitat and Wasson Lakes that we derived from dendrochronology. While the corroboration of landslide age with ^{14}C dating proves useful, our results also demonstrate the limitations of ^{14}C methods for dating landslides with high

accuracy. Our radiocarbon results provide an uncertainty of landslide age spanning >6,000 years at Klickitat Lake and >8,000 years at Wasson Lake. The issue of inheritance of older carbon in landslide deposits highlights the potential for long residence times to bias landslide age estimates based on detrital samples collected from landslide deposits. Large or particularly resilient material that takes longer to decay may exist on the Earth's surface for decades and potentially much longer prior to landslide emplacement (Figures 9, 10). Our data demonstrate that this is the case for detrital charcoal. The general practice when collecting detrital organic material from a landslide deposit for radiocarbon analysis often fails to account for factors that likely affect the calculated age; the assumption that the age of detrital material in a landslide is the same as the landslide relies on several key assumptions, many of which are not always valid. Specifically, sampling larger wood from a landslide must concede that the wood may be much older than the landslide, as the interior wood of a tree must pre-date the time of death by many years and perhaps even centuries (Gavin, 2001; Trumbore, 2000). This is particularly true if the outer rings of the tree are missing or otherwise not available for sampling, which is not always obvious at the time of sample collection (Clague, 2015). Further, if the tree died prior to landslide failure, its residence time on the landscape remains unknown (Clague, 2015; Gavin 2003). In addition, the residence time of organic material, including pine needles and cones and leaves, on hillslopes may sometimes be remarkably long, spanning centuries for wood to millennia for charcoal (Figures 9, 10). Long residence times may be increasingly likely for materials that are buried deeper in the soil column (Trumbore, 2000). Hence, assuming no contamination of younger carbon in a landslide deposit via bioturbation, for example, landslide ages derived from ^{14}C dating of deposits should be considered a maximum age.

The issue of residence time on the landscape becomes less relevant for dating very old landslides because the proportion of the residence time to landslide age shrinks. In addition, for landslide ages that correspond to linear portions of the radiocarbon calibration curve (few 'wiggles'), including >500 yrs. B.P., uncertainty will be lower. However, as landslide age decreases, the importance of residence time increases because the residence time of datable detritus may be greater than the age of the landslide. In addition, for landslides that occurred <500 yrs. B.P., the intense oscillation in the radiocarbon calibration curve increases uncertainty of derived ages (Figure 8). If analyses are exclusively derived from charcoal, landslide ages appear to be significantly older, as we demonstrate at Klickitat and Wasson Lakes. Charcoal-derived ages suggest that Klickitat Lake formed up to 6,300 years ago and Wasson Lake formed up to 9,100 years ago (Figures 9, 10), which contradicts our dendrochronology ages by millennia. Radiocarbon dating charcoal provides the age of the wood when the fire that burned the wood occurred (Gavin, 2003, 2001; Pessenda et al., 2001; Scharer et al., 2011; Trumbore, 2000), and that charcoal can persist in the landscape for millennia.

In landslide-dam lakes where drowned, standing snags are absent or poorly preserved, sampling buried trees in landslide deposits can be conducted to minimize systematic bias. For example, collection of large wood fragments without context invites high uncertainty, as the inner rings of a tree may be significantly older than the landslide event. Depending on the quality of the preserved wood, dendrochronological analysis of buried trees in landslide deposits can provide highly accurate estimates of landslide age (e.g., Bégin and Filion, 1988; Fillion et al., 1991). In addition, bark should be avoided for ^{14}C dating, as it grows slowly and incorporates organic material throughout the life of the tree, often resulting in an older calculated age (Atwater, pers. comm., 2017; Gavin, pers. comm., 2018). We encountered this problem when attempting to use bark for preliminary dating of snags at Wasson and Klickitat Lakes; ^{14}C ages from bark of the standing snags in Wasson Lake produced ages

approximately 200 years too old (Figure 10). While bark from Klickitat Lake provided ages that bracket the true age of 1751 AD, the location of the ages on the radiocarbon calibration curve provides an ambiguous date, with 1751 AD being only one of many possible ages (Figure 9). Given these potential complications when dating a landslide using radiocarbon, great care should be taken to sample material that will derive the age most likely to be contemporaneous with landslide occurrence.

Calibration of Other Landslide Dating Techniques

Dendrochronology provides landslide ages with sub-annual accuracy, a capability currently unmatched by other dating techniques. However, dating methods such as radiocarbon, tephrochronology, landslide creep rates, and surface roughness dating are more widely used given the limited settings in which dendrochronology is applicable (Booth et al., 2018, 2017; Cerovski-Darriau et al., 2014; Clague, 2015; LaHusen et al., 2016; Leithold et al., 2018; Schulz et al., 2012). Calibration of these methods with the landslide ages that we derived by dendrochronological means may facilitate the use and testing of these techniques, particularly in forested landscapes subject to similar geomorphic processes as the OCR.

Calibration of the surface roughness dating technique by dendrochronology could greatly enhance its utility, especially if a large suite of landslide-ages from dendrochronology could be used to refine a surface roughness calibration curve for western Oregon (Booth et al., 2017, 2009; LaHusen et al., 2016). Surface roughness dating could then be applied to numerous landslides in western Oregon of variable size and morphology. Clarification of the frequency and magnitude of recent landslides (<1 kyr) will improve assessments of modern landslide hazards, and dating of the oldest landslides from soil residence times or exposure ages will be useful for studies of landscape evolution in the OCR (e.g., Almond et al., 2007).

To preliminarily determine if surface roughness is a good indicator of landslide age in the OCR, we calculated the surface roughness (standard deviation of slope) of the landslides at Klickitat and Wasson Lakes. Using a 15-meter moving window, we found average surface roughness values of 4.4 at Klickitat Lake and 7.3 at Wasson Lake. These values indicate lower roughness at Klickitat Lake and higher roughness at Wasson Lake, which is consistent with the older age of Klickitat Lake. We compared these surface roughness values to the roughness-age calibration curve of LaHusen et al. (2016) and found that the roughness of the landslide at Wasson Lake is consistent with a landslide age of 1819 AD. The low roughness of the landslide at Klickitat Lake, however, suggests a landslide age of ~7000 B.P., much older than the calculated age of 1751 AD. Therefore, calibration of the roughness-age curve for the OCR is necessary, as our data thus far are not consistent with roughness-age curves constructed in different lithologies (LaHusen et al., 2016). Further, the landslides that form Klickitat and Wasson Lakes, while large, do not exhibit the same deep-seated morphology as the landslides that often define entire hillslopes throughout the OCR (Cruden and Varnes, 1996; Roering et al., 2005). The Klickitat and Wasson landslides are morphologically more consistent with large flow-like failures, as their form is elongate and they appear to have had a more fluid and longer runout (Cruden and Varnes, 1996). The scale of these landslides also complicates measurement of surface roughness, as bare earth lidar data resolution on heavily vegetated landslides in the OCR results in low point densities that potentially artificially introduce erroneous surface roughness. If surface roughness dating is to be used in the OCR to constrain forcing mechanisms and provide targeted sites for dendrochronology, additional work is needed to constrain how lithology and landslide style influence morphology that provides the basis for age-roughness curves. In addition, re-filtering of lidar data is necessary at some sites to ensure sufficient ground coverage.

The ages that we calculated from sediment infilling at Klickitat and Wasson Lakes bracket the ages determined from dendrochronology. The volume of alluvial sediment that filled in the valleys upstream from the landslide dams is useful beyond simply corroborating the dendrochronology-derived landslide ages. Assuming prior knowledge of erosion rate and pre-landslide topography, calculating landslide ages from sediment infilling could be applied rapidly to sites throughout Cascadia. Initial calculation of ages with sediment infilling may pinpoint sites suitable for targeted dendrochronological analysis, especially if searching for landscape response to a specific triggering event, such as the 1700 AD earthquake. However, confirming that dams trap sediments is necessary because infilled dams that do not store sediments are poor recorders of sedimentation. In addition, the alluvial record preserved upstream of landslide dams is an effective tool for extracting paleoclimate, biotic, and surface process records (e.g., Mackey et al., 2011; Marshall et al., 2017; Morey et al., 2013; Richardson et al., 2018).

The complementary nature of radiocarbon, tephrochronology, creep rates, sediment infilling, and surface roughness dating methods with dendrochronology is useful because dendrochronology, while more accurate, is more time-intensive, and limited to sites with standing snags. The ability of techniques, such as sediment infilling and surface roughness dating, to generate age estimates for large portions of the landscape in Cascadia allows for targeted dendrochronology field work and investigation of spatial patterns that may relate to seismic triggering or other forcing mechanisms.

Improved Dating of Existing Landslide Ages

Standing Douglas-fir snags at landslide-dammed lakes not only provide high accuracy ages for landslides, but also extend existing tree ring chronologies for the region, which increases the temporal reach of paleoclimate studies in Cascadia and improves the probability of dating older landslides. While using dendrochronology to date landslides is not applicable in locations where trees are not available, it may be a viable dating mechanism at some locations to constrain the age of landslides. For example, Leithold et al. (2018) provide a single radiocarbon age for a sub-aerial landslide in the Olympic Mountains, Washington, and posit that it may be connected to the 1700 AD Cascadia earthquake. For their radiocarbon analysis, they collected wood from the outermost ring of a snag found in a terrace deposit adjacent to the landslide. For sites such as these, it may be possible to crossdate the tree ring timeseries from the snag and neighboring snags with existing chronologies in the region to better constrain the age of that landslide (Leithold, pers. comm. 2018). Similarly, other large landslides with established ages in the OCR may have heretofore unidentified standing snags that may help either constrain the age of the landslide, or if too old for crossdating with existing chronologies, provide important data on paleoclimate in the region. As more landslides, specifically in a single region, are dated with high-accuracy dendrochronological methods, existing tree ring chronologies will continue to be extended, improving the possibility of dating even older landslides.

CONCLUSIONS

We exploited the ubiquitous signature of deep-seated landslides in the OCR to investigate seismic and climatic forcings on the Cascadia landscape. Using ‘ghost forests’ at landslide-dammed lakes in the OCR, we calculated sub-annually accurate landslide ages including the winter of 1751/52 AD and the winter of 1819/20 AD at Klickitat and Wasson Lakes, respectively. Even though we have yet to link the 1700 AD earthquake with landsliding, the high-accuracy ages that we have derived for landslides in the OCR allows for in-depth investigation of slope-triggering mechanisms, including severe climatic forcings as well as earthquake triggered landslide initiation followed by delayed catastrophic failure. In addition, development of extended tree-ring chronologies from standing snags at landslide-

dammed lakes, in conjunction with existing chronologies in western Oregon, will provide key constraints on the regional climate in Cascadia throughout the last 600 or more years.

While dendrochronology provides high, often sub-annual, accuracy dating of landslides, ghost forests are not common features. We have demonstrated that the variance of ages for detrital ^{14}C dating of landslides can be large, up to 6,000 years at Klickitat Lake and almost 9,000 years at Wasson Lake; however, cautious and redundant sampling of landslide detritus for ^{14}C analysis will increase the probability of obtaining a representative age. In addition, sediment infilling calculations of landslide age are useful for pinpointing sites for future targeted dendrochronological studies, as our results from sediment infilling rates bracket dendrochronology-derived landslide ages. Hence, traditional methods, such as ^{14}C dating, sediment infill dating, and surface roughness dating are key tools for determining landslide ages. Calibration of these methods using dendrochronology will promote more accurate ages, particularly in regions that are subject to similar surface processes as the OCR. These enhanced dating techniques may then be used to construct a landslide age database for western Oregon, which will allow for testing of both seismic and climatic triggering mechanisms on slope stability in Cascadia.

ACKNOWLEDGMENTS

This research was funded by a National Earthquake Hazards Reduction Program (NEHRP) grant . ^{14}C analyses were completed at the mass spectrometry labs at Lawrence Livermore National Laboratory and the University of Arizona. We thank Jay Sexton and Dennis Fletcher for sampling assistance and Sean LaHusen, Marisa Acosta, Jerod Aguilar, Nick Candusso, Elizabeth Curtiss, Aly Ervin, Justin McCarley, Samuel Nath, Ethan Niyangoda, Nicco Ryan, Ray Weldon, and the UO 2016 Neotectonics class for additional field and sample preparation help. Conversations with Brian Atwater, Alison Duvall, Dan Gavin, Pat Pringle, and Harvey Kelsey were particularly helpful.

THE FOLLOWING PUBLICATIONS RESULTED FROM THE WORK PERFORMED UNDER THIS AWARD:

Lahusen, S., A.R. Duvall, A.M. Booth, A. Grant, J. Wartman, W. Struble, J. Roering, and D. Montgomery, (2018), Megathrust Earthquakes and Coseismic Landslides in Cascadia: Insights from a New Inventory of Thousands of Landslides Dated Using Calibrated Surface Roughness, *AGU Fall Mtg, Washington, D.C. (SEE ABSTRACT AT END OF THIS REPORT)*

Struble, W., J.J. Roering, B. Black, W. Burns, N. Calhoun, and L. Wetherell, (in review), Dendrochronological dating of landslides in western Oregon: Searching for signals of the Cascadia 1700 AD earthquake, *Geological Society of America Bulletin. (THIS REPORT)*

REFERENCES CITED

Allstadt, K., Vidale, J.E., Frankel, A.D., 2013. A Scenario Study of Seismically Induced Landsliding in Seattle Using Broadband Synthetic Seismograms. Bulletin of the Seismological Society of America 103, 2971–2992. doi: 10.1785/0120130051

Almond, P., Roering, J., Hales, T.C., 2007. Using soil residence time to delineate spatial and temporal patterns of transient landscape response. Journal of Geophysical Research 112. doi: 10.1029/2006JF000568

Atwater, B.F., 2017. Personal communication.

Atwater, B.F., Satoko, M.-R., Kenji, S., Yoshinobu, T., Kazue, U., Yamaguchi, D.K., 2005. The orphan tsunami of 1700: Japanese clues to a parent earthquake in North America. USGS Professional Paper 1707.

Atwater, B.F., Yamaguchi, D.K., 1991. Sudden, probably coseismic submergence of Holocene trees and grass in coastal Washington State. Geology 19, 706–709.

Balco, G., Finnegan, N., Gendaszek, A., Stone, J.O., Thompson, N., 2013. Erosional response to northward-propagating crustal thickening in the coastal ranges of the US Pacific Northwest. American Journal of Science 313, 790–806.

Baldwin, E.M., 1956. Geologic map of the lower Siuslaw River area, Oregon, scale 1:62 500, 1 sheet.

Ballantyne, C.K., Stone, J.O., 2004. The Beinn Alligin rock avalanche, NW Scotland: cosmogenic 10Be dating, interpretation and significance. The Holocene 14, 448–453. doi: 10.1191/0959683604hl720rr

Bégin, C., Filion, L., 1988. Age of landslides along Grande Riviére de la Baleine estuary, eastern coast of Husdon Bay, Quebec (Canada). Boreas 17, 289-299.

Bekker, M.F., Metcalf, D.P., Harley, G.L., 2018. Hydrology and Hillslope Processes Explain Spatial Variation in Tree-Ring Responses to the 1983 Earthquake at Borah Peak, Idaho, USA: Borah Peak Earthquake Tree-Ring Responses. Earth Surface Processes and Landforms. doi: 10.1002/esp.4470

Benda, L., 1990. The influence of debris flows on channels and valley floors in the Oregon Coast Range, USA. Earth Surface Processes and Landforms 15, 457–466.

Benda, L., Dunne, T., 1997. Stochastic forcing of sediment supply to channel networks from landsliding and debris flow. Water Resources Research 33, 2849–2863. doi: 10.1029/97WR02388

Beschta, R.L., 1978. Long-term patterns of sediment production following road construction and logging in the Oregon Coast Range. Water Resources Research 14, 1011–1016. doi: 10.1029/WR014i006p01011

Bierman, P., Clapp, E., Nichols, K., Gillespie, A., Caffee, M.W., 2001. Using cosmogenic nuclide measurements in sediments to understand background rates of erosion and sediment transport. Landscape Erosion and Evolution Modleing. Springer, pp. 89-115.

Black, B.A., Dunham, J.B., Blundon, B.W., Brim-Box, J., Tepley, A.J., 2015. Long-term growth-increment chronologies reveal diverse influences of climate forcing on freshwater and forest biota in the Pacific Northwest. Global Change Biology 21, 594–604. doi: 10.1111/gcb.12756

Booth, A.M., LaHusen, S.R., Duvall, A.R., Montgomery, D.R., 2017. Holocene history of deep-seated landsliding in the North Fork Stillaguamish River valley from surface roughness analysis, radiocarbon dating, and numerical landscape evolution modeling. Journal of Geophysical Research: Earth Surface 122, 456–472. doi: 10.1002/2016JF003934

Booth, A.M., McCarley, J., Hinkle, J., Shaw, S., Ampuero, J.-P., Lamb, M.P., 2018. Transient Reactivation of a Deep-Seated Landslide by Undrained Loading Captured With Repeat Airborne and Terrestrial Lidar. Geophysical Research Letters 45, 4841–4850. doi: 10.1029/2018GL077812

Booth, A.M., Roering, J.J., Perron, J.T., 2009. Automated landslide mapping using spectral analysis and high-resolution topographic data: Puget Sound lowlands, Washington, and Portland Hills, Oregon. Geomorphology 109, 132–147. doi: 10.1016/j.geomorph.2009.02.027

Braitseva, O.A., Sulerzhitsky, L.D., Litasova, S.N., Melekestsev, I.V., Ponomareva, V.V., 1993. 1595-1845-1-PB.pdf. Radiocarbon 35, 463–476.

Brown, G.W., Krygier, J.T., 1971. Clear-Cut Logging and Sediment Production in the Oregon Coast Range. Water Resources Research 7, 1189–1198. doi: 10.1029/WR007i005p01189

Burns, W.J., Duplantis, S., Jones, C.B., English, J.T., 2012. Lidar data and Landslide Inventory Maps of the North Fork Siuslaw River and Big Elk Creek Watersheds, Lane, Lincoln, and Benton Counties.

Burns, W.J., Madin, I.P., 2009. Protocol for Inventory Mapping of Landslide Depostits from Light Detection and Ranging (Lidar) Imagery (Special Paper 42). Oregon Department of Geology and Mineral Industries.

Burns, W.J., Watzig, R., 2014. Statewide Landslide Information Database of Oregon Release-3.0, Oregon Department of Geology and Mineral Industries, SLIDO-3.0. Oregon Department of Geology and Mineral Industries, SLIDO-3.0.

Butterfield, N., J., Bunds, M.P., Zanazzi, A., Toke, N.A., 2015. A preliminary look at geomorphic impacts and timing of two large, drainage-damming landslides in the central Wasatch. Presented at the GSA 2015 Annual Meeting.

Cerovski-Darriau, C., Roering, J.J., Marden, M., Palmer, A.S., Bilderback, E.L., 2014. Quantifying temporal variations in landslide-driven sediment production by reconstructing paleolandscapes using tephrochronology and lidar: Waipaoa River, New Zealand. Geochemistry, Geophysics, Geosystems 15, 4117–4136. doi: 10.1002/2014GC005467

Clague, J.J., 2015. Paleolandslides, in: Landslide Hazards, Risks and Disasters. Elsevier, pp. 321–344. doi: 10.1016/B978-0-12-396452-6.00010-0

Cruden, D.M., Varnes, D.J., 1996. Landslide types and processes, in Landslides-Investigation and Mitigation, edited by A.K. Turner and R.L. Schuster, pp. 36-75, Special Report 247, Transport. Res. Board, National Res. Council, National Academic Press, Washington, DC.

Dadson, S.J., Hovius, N., Chen, H., Dade, W.B., Lin, J.-C., Hsu, M.-L., Lin, C.-W., Horng, M.-J., Chen, T.-C., Milliman, J., others, 2004. Earthquake-triggered increase in sediment delivery from an active mountain belt. Geology 32, 733–736.

Danišík, M., Shane, P., Schmitt, A.K., Hogg, A., Santos, G.M., Storm, S., Evans, N.J., Keith Fifield, L., Lindsay, J.M., 2012. Re-anchoring the late Pleistocene tephrochronology of New Zealand based on concordant radiocarbon ages and combined 238U/230Th disequilibrium and (U–Th)/He zircon ages. Earth and Planetary Science Letters 349–350, 240–250. doi: 10.1016/j.epsl.2012.06.041

Densmore, A.L., Hovius, N., 2000. Topographic fingerprints of bedrock landslides. Geology 4, 371-374.

Dietrich, W.E., Dunne, T., 1978. Sediment budget for a small catchment in mountainous terrain. Zeitschrift für Geomorphologie N.F. 29, 191–206. doi: 10.1007/s10069-002-0008-0

DOGAMI, 2012, Central Coast Lidar Project 2011, Oregon Lidar Consortium, distributed by Oregon Department of Geology and Mineral Industries Lidar Program airborne lidar survey.

DOGAMI, 2015, Upper Umpqua 3DEP, Oregon Lidar Consortium, distributed by Oregon Department of Geology and Mineral Industries Lidar Program airborne lidar survey.

Douglass, A.E., 1941. Crossdating in Dendrochronology. Journal of Forestry 39, 825–831.

Dumitru, T.A., Ernst, W.G., Wright, J.E., Wooden, J.L., Wells, R.E., Farmer, L.P., Kent, A.J.R., Graham, S.A., 2013. Eocene extension in Idaho generated massive sediment floods into the Franciscan trench and into the Tyee, Great Valley, and Green River basins. Geology 41, 187–190. doi: 10.1130/G33746.1

Fantucci, R., McCord, A., 1995. Reconstruction of landslide dynamics with dendrochronological methods. Dendrochronologia 13, 43–58.

Filion, L., Quinty, F., Bégin, C., 1991. A chronology of landslide activity in the valley of Riviére du Gouffre, Charlevoix, Quebec. Canadian Journal of Earth Science 28, 250-256.

Gadgil, P.D., 1971. Effect of waterlogging on mycorrhizas of radiata pine and Douglas fir. New Zealand Journal of Forestry Science 2, 5.

Gallen, S.F., Clark, M.K., Godt, J.W., Roback, K., Niemi, N.A., 2016. Application and evaluation of a rapid response earthquake-triggered landslide model to the 25 April 2015 Mw 7.8 Gorkha earthquake, Nepal. Tectonophysics. doi: 10.1016/j.tecto.2016.10.031

Gavin, D.G., 2001. Estimation of inbuilt age in radiocarbon ages of soil charcoal for fire history studies. Radiocarbon 43, 27-44. doi: 10.1017/S003382220003160X

Gavin, D.G., 2003. Forest soil disturbance intervals inferred from soil charcoal radiocarbon dates. Canadian Journal of Forest Research 33, 2514–2518. doi: 10.1139/x03-185

Gavin, D.G., 2018. Personal communication.

Goldfinger, C., Nelson, C.H., Morey, A.E., Johnson, J.E., Patton, J.R., Karabanov, E., Gutierrez-Pastor, J., Eriksson, A.T., Gracia, E., Dunhill, G., 2012. Turbidite event history: Methods and implications for Holocene paleoseismicity of the Cascadia subduction zone. US Geological Survey Professional Paper 1661, 170.

Gorum, T., Korup, O., van Westen, C.J., van der Meijde, M., Xu, C., van der Meer, F.D., 2014. Why so few? Landslides triggered by the 2002 Denali earthquake, Alaska. Quaternary Science Reviews 95, 80–94. doi: 10.1016/j.quascirev.2014.04.032

Heimsath, A.M., Dietrich, W.E., Nishiizumi, K., Finkel, R.C., 2001. Stochastic processes of soil production and transport: erosion rates, topographic variation and cosmogenic nuclides in the Oregon Coast Range. Earth Surface Processes and Landforms 26, 531–552. doi: 10.1002/esp.209

Heller, P.L., Dickinson, W.R., 1985. Submarine Ramp Facies Model for Delta-Fed, Sand-Rich Turbidite Systems. AAPG Bulletin 69. doi: 10.1306/AD462B37-16F7-11D7-8645000102C1865D

Heller, P.L., Peterman, Z.E., O'Neil, J.R., Shafiqullah, M., 1985. Isotopic provenance of sandstones from the Eocene Tyee Formation, Oregon Coast Range. Geological Society of America Bulletin 96, 770. doi: 10.1130/0016-7606(1985)96

Heller, P.L., Ryberg, P.T., 1983. Sedimentary record of subduction to forearc transition in the rotated Eocene basin of western Oregon. Geology 11, 380. doi: 10.1130/0091-7613(1983)11

Hovius, N., Meunier, P., Lin, C.-W., Chen, H., Chen, Y.-G., Dadson, S., Horng, M.-J., Lines, M., 2011. Prolonged seismically induced erosion and the mass balance of a large earthquake. Earth and Planetary Science Letters 304, 347–355. doi: 10.1016/j.epsl.2011.02.005

Ivy-Ochs, S., Poschinger, A. v., Synal, H.-A., Maisch, M., 2009. Surface exposure dating of the Flims landslide, Graubünden, Switzerland. Geomorphology 103, 104–112. doi: 10.1016/j.geomorph.2007.10.024

Jibson, R., Allstadt, K., Rengers, F., Godt, J., 2018. Overview of the Geologic Effects of the November 14, 2016, Mw 7.8 Kaikoura, New Zealand, Earthquake: U.S. Geological Survey Scientific Investigations Report No. 2017–5146.

Jibson, R.W., Harp, E.L., Michael, J.A., 2000. A method for producing digital probabilistic seismic landslide hazard maps. Engineering Geology 58, 271–289.

Kargel, J.S., Leonard, G.J., Shugar, D.H., Haritashya, U.K., Bevington, A., Fielding, E.J., Fujita, et al., 2016. Geomorphic and geologic controls of geohazards induced by Nepal's 2015 Gorkha earthquake. Science 351, 8353–8353. doi: 10.1126/science.aac8353

Karlin, R.E., Holmes, M., Abella, S.E.B., Sylwester, R., 2004. Holocene landslides and a 3500-year record of Pacific Northwest earthquakes from sediments in Lake Washington. Geological Society of America Bulletin 116, 94–108.

Keefer, D.K., 2002. Investigating landslides caused by earthquakes–a historical review. Surveys in geophysics 23, 473–510.

Keefer, D.K., 1984. Landslides caused by earthquakes. Geological Society of America Bulletin 95, 406–421.

Kelsey, H.M., Bockheim, J.G., 1994. Coastal landscape evolution as a function of eustasy and surface uplift rate, Cascadia margin, southern Oregon. Geological Society of America Bulletin 106, 840–854. doi: 10.1130/0016-

Kelsey, H.M., Engebretson, D.C., Mitchell, C.E., Ticknor, R.L., 1994. Topographic form of the Coast Ranges of the Cascadia Margin in relation to coastal uplift rates and plate subduction. Journal of Geophysical Research 99, 12245–12255.

Kelsey, H.M., Ticknor, R.L., Bockheim, J.G., Mitchell, E., 1996. Quaternary upper plate deformation in coastal Oregon. Geological Society of America Bulletin 108, 843–860.

LaHusen, S.R., Duvall, A.R., Booth, A.M., Montgomery, D.R., 2016. Surface roughness dating of long-runout landslides near Oso, Washington (USA), reveals persistent postglacial hillslope instability. Geology 44, 111–114.

Lang, A., Moya, J., Corominas, J., Schrott, L., Dikau, R., 1999. Classic and new dating methods for assessing the temporal occurrence of mass movements. Geomorphology 30, 33–52. doi: 10.1016/S0169-555X(99)00043-4

Larsen, I.J., Montgomery, D.R., Korup, O., 2010. Landslide erosion controlled by hillslope material. Nature Geoscience 3, 247-251. doi: 10.1038/ngeo776.

Larsson, L., 2013. CooRecorder and CDendro programs of the CooRecorder /CDendro package version 9.0.

Leithold, E.L., 2018. Personal communication.

Leithold, E.L., Wegmann, K.W., Bohnenstiehl, D.R., Smith, S.G., Noren, A., O'Grady, R., 2018. Slope failures within and upstream of Lake Quinault, Washington, as uneven responses to Holocene earthquakes along the Cascadia subduction zone. Quaternary Research 89, 178–200. doi: 10.1017/qua.2017.96

Li, G., West, A.J., Densmore, A.L., Jin, Z., Parker, R.N., Hilton, R.G., 2014. Seismic mountain building: Landslides associated with the 2008 Wenchuan earthquake in the context of a generalized model for earthquake volume balance. Geochemistry, Geophysics, Geosystems 15, 833–844. doi: 10.1002/2013GC005067

Mackey, B.H., Roering, J.J., Lamb, M.P., 2011. Landslide-dammed paleolake perturbs marine sedimentation and drives genetic change in anadromous fish. Proceedings of the National Academy of Sciences 108, 18905–18909. doi: 10.1073/pnas.1110445108

Madin, I.P., Burns, W.J., 2013. Ground motion, ground deformation, tsunami inundation, coseismic subsidence, and damage potential maps for the 2012 Oregon Resilience Plan for Cascadia Subduction Zone Earthquakes: Oregon Department of Geology and Mineral Industries Open-File report O-13-06.

Marc, O., Hovius, N., Meunier, P., 2016. The mass balance of earthquakes and earthquake sequences: The Mass Balance of Earthquakes. Geophysical Research Letters 43, 3708–3716. doi: 10.1002/2016GL068333

Marc, Odin, Hovius, N., Meunier, P., Gorum, T., Uchida, T., 2016. A seismologically consistent expression for the total area and volume of earthquake-triggered landsliding. Journal of Geophysical Research: Earth Surface 121, 640–663. doi: 10.1002/2015JF003732

Marshall, J.A., Roering, J.J., Bartlein, P.J., Gavin, D.G., Granger, D.E., Rempel, AW., Praskievicz, S.J., Hales, T.C., 2015. Frost for the trees: Did climate increase erosion in unglaciated landscapes during the late Pleistocene? Science Advances 1, e1500715-e1500715. doi: 10.1126/sciadv.1500715

Marshall, J.A., Roering, J.J., Gavin, D.G., Granger, D.E., 2017. Late Quaternary climatic controls on erosion rates and geomorphic processes in western Oregon, USA. Geological Society of America Bulletin 129, 715–731. doi: 10.1130/B31509.1

Massey, C., Townsend, D., Rathie, E., Allstadt, K.E., Lukovic, B., Kaneko, Y., et al., 2018. Landslides triggered by the 14 November 2016 M_w 7.8 Kaikōura Earthquake, New Zealand. Bulletin of the Seismological Society of America 108, 1630-1648.

May, C., Roering, J., Eaton, L.S., Burnett, K.M., 2013. Controls on valley width in mountainous landscapes: The role of landsliding and implications for salmonid habitat. Geology 41, 503–506. doi: 10.1130/G33979.1

McKean, J., Roering, J., 2004. Objective landslide detection and surface morphology mapping using high-resolution airborne laser altimetry. Geomorphology 57, 331–351. doi: 10.1016/S0169-555X(03)00164-8

McNeill, L.C., Kulm, L.D., Yeats, R.S., 2000. Tectonics of the Neogene Cascadia forearc basin: Investigations of a deformed late Miocene unconformity. Geological Society of America Bulletin 16.

Meunier, P., Hovius, N., Haines, A.J., 2007. Regional patterns of earthquake-triggered landslides and their relation to ground motion. Geophysical Research Letters 34. doi: 10.1029/2007GL031337

Meunier, P., Hovius, N., Haines, J.A., 2008. Topographic site effects and the location of earthquake induced landslides. Earth and Planetary Science Letters 275, 221–232. doi: 10.1016/j.epsl.2008.07.020

Montgomery, D.R., 2001. Slope distributions, threshold hillslopes, and steady-state topography. American Journal of Science 301, 432–454.

Montgomery, D.R., Schmidt, K.M., Dietrich, W.E., Greenberg, H., 2000. Forest clearing and regional landsliding. Geology 28, 311-314.

Morey, A.E., Goldfinger, C., Briles, C.E., Gavin, D.G., Colombaroli, D., Kusler, J.E., 2013. Are great Cascadia earthquakes recorded in the sedimentary records from small forearc lakes? Natural Hazards and Earth System Science 13, 2441–2463. doi: 10.5194/nhess-13-2441-2013

Newmark, N.M., 1965. Effects of earthquakes on dams and embankments. Geotechnique 15, 139–160.

Olsen, M.J., Ashford, S.A., Mahlingam, R., Sharifi-Mood, M., O'Banion, M., Gillins, D.R., 2015. Impacts of potential seismic landslides on lifeline corridors. Final Report SPR 740. Oregon DOT, Salem, Federal Highway Administration, Washington, DC, 238 pp.

Penserini, B.D., Roering, J.J., Streig, A., 2017. A morphologic proxy for debris flow erosion with application to the earthquake deformation cycle, Cascadia Subduction Zone, USA. Geomorphology 282, 150–161. doi: 10.1016/j.geomorph.2017.01.018

Personius, S.F., 1995. Late Quaternary stream incision and uplift in the forearc of the Cascadia subduction zone, western Oregon. Journal of Geophysical Research: Solid Earth 100, 20193–20210. doi: 10.1029/95JB01684

Pessenda, L.C.R., Gouveia, S.E.M., Aravena, R., 2001. Radiocarbon Dating of Total Soil Organic Matter and Humin Fraction and Its Comparison with 14C Ages of Fossil Charcoal. Radiocarbon 43, 595–601. doi: 10.1017/S0033822200041242

Pringle, P.T., 2014. Buried and Submerged Forests of Washington and Oregon: Time Capsules of Environmental and Geologic History. Western Forester 59, 14–15, 22.

PRISM Climate Group, 2016. PRISM Climate Group: Oregon State University.

Ramsey, C.B., 2017. Methods for summarizing radiocarbon datasets. Radioccarbon 59, 1809-1833.

Ramsey, C.B., 2009. Bayesian analysis of radiocarbon dates. Radiocarbon 51, 337–360.

Ramsey, C.B., 1995. Radiocarbon Calibration and Analysis of Stratigraphy: The OxCal Program. Radiocarbon 37, 425–430. doi: 10.1017/S0033822200030903

Reimer, P.J., Baillie, M.G., Bard, E., Bayliss, A., Beck, J.W., Blackwell, P.G., Ramsey, C.B., Buck, C.E., Burr, G.S., Edwards, R.L., 2009. IntCal09 and Marine09 radiocarbon age calibration curves, 0–50,000 years cal BP. Radiocarbon 51, 1111–1150.

Reimer, P.J., Bard, E., Bayliss, A., Beck, J.W., Blackwell, P.G., Ramsey, C.B., Buck, C.E., et al., 2013. IntCal13 and Marine 13 radiocarbon age calibration curves 0-50,000 years cal BP. Radiocarbon, 55, 1869-1887.

Reneau, S.L., Dietrich, W.E., 1991. Erosion rates in the southern Oregon Coast Range: Evidence for an equilibrium between hillslope erosion and sediment yield. Earth Surface Processes and Landforms 16, 307–322.

Reneau, S.L., Dietrich, W.E., Dorn, R.I., Berger, C.R., Rubin, M., 1986. Geomorphic and paleoclimatic implications of latest Pleistocene radiocarbon dates from colluvium-mantled hollows, California. Geology 14, 655. doi: 10.1130/0091-7613(1986)

Richardson, K.N.D., Hatten, J.A., Wheatcroft, R.A., 2018. 1500 years of lake sedimentation due to fire, earthquakes, floods and land clearance in the Oregon Coast Range: geomorphic sensitivity to floods during timber harvest period: Natural and anthropogenic effects on sedimentation in an Oregon lake. Earth Surface Processes and Landforms 43, 1496–1517. doi: 10.1002/esp.4335

Roback, K., Clark, M.K., West, A.J., Zekkos, D., Li, G., Gallen, S.F., Chamlagain, D., Godt, J.W., 2017. The size, distribution, and mobility of landslides caused by the 2015 M w 7.8 Gorkha earthquake, Nepal. Geomorphology 301, 121–138. doi: 10.1016/j.geomorph.2017.01.030

Robison, E.G., Mills, K., Paul, J., Dent, L., Skaugset, A., 1999. Storm impacts and landslides of 1996: Oregon Department of Forestry Forest Practices Technical Final Report 4, 145 pp.

Roering, J.J., Kirchner, J.W., Dietrich, W.E., 2005. Characterizing structural and lithologic controls on deep-seated landsliding: Implications for topographic relief and landscape evolution in the Oregon Coast Range, USA. Geological Society of America Bulletin 117, 654. doi: 10.1130/B25567.1

Scharer, K.M., Biasi, G.P., Weldon, R.J., 2011. A reevaluation of the Pallett Creek earthquake chronology based on new AMS radiocarbon dates, San Andreas fault, California. Journal of Geophysical Research 116. doi: 10.1029/2010JB008099

Schmidt, K.M., Montgomery, D.R., 1995. Limits to Relief. Science 270, 617–620.

Schulz, W.H., Galloway, S.L., Higgins, J.D., 2012. Evidence for earthquake triggering of large landslides in coastal Oregon, USA. Geomorphology 141–142, 88–98. doi: 10.1016/j.geomorph.2011.12.026

Schuster, R.L., Logan, R.L., Pringle, P.T., 1992. Prehistoric Rock Avalanches in the Olympic Mountains, Washington. Science 258, 1620–1621.

Stefanini, M.C., 2004. Spatio-temporal analysis of a complex landslide in the Northern Apennines (Italy) by means of dendrochronology. Geomorphology 63, 191–202. doi: 10.1016/j.geomorph.2004.04.003

Stock, J., Dietrich, W.E., 2003. Valley incision by debris flows: Evidence of a topographic signature: valley incision by debris flows. Water Resources Research 39. doi: 10.1029/2001WR001057

Tanyaş, H., Allstadt, K.E., van Westen, C.J., 2018. An updated method for estimating landslide-event magnitude: An updated method for estimating landslide-event magnitude. Earth Surface Processes and Landforms 43, 1836–1847. doi: 10.1002/esp.4359

Tanyaş, H., van Westen, C.J., Allstadt, K.E., Anna Nowicki Jessee, M., Görüm, T., Jibson, R.W., Godt, J.W., Sato, H.P., Schmitt, R.G., Marc, O., Hovius, N., 2017. Presentation and Analysis of a Worldwide Database of Earthquake-Induced Landslide Inventories: Earthquake-Induced Landslide Inventories. Journal of Geophysical Research: Earth Surface 122, 1991–2015. doi: 10.1002/2017JF004236

Thrall, G.F., Jack, R., Johnson, J.J., Stanley, D.A., 1980. Failure mechanisms of the Drift Creek Slide, in: Geological Society of America. Presented at the Abstract with Programs, p. 156.

Trumbore, S.E., 2000. Radiocarbon geochronology, in: Noller, J.S., Sowers, J.M., Lettis, W.R. (Eds.), AGU Reference Shelf. American Geophysical Union, Washington, D. C., pp. 41–60. doi: 10.1029/RF004p0041

United States Department of Agriculture (USDA), 2000, National Agriculture Imagery Program (NAIP) for the Farm Service Agency's (FSA), Oregon Imagery Framework Implementation Team.

Valagussa, A., Marc, O., Frattini, P., Crosta, G.B., 2019. Seismic and geological controls on earthquake-induced landslide size. Earth and Planetary Science Letters 506, 268-281.

Veblen, T.T., Ashton, D.H., 1978. Catastrophic influences on the vegetation of the Valdivian Andes, Chile. Vegetatio 36, 149–167. doi: 10.1007/BF02342598

Wartman, J., Dunham, L., Tiwari, B., Pradel, D., 2013. Landslides in Eastern Honshu Induced by the 2011 Tohoku Earthquake. Bulletin of the Seismological Society of America 103, 1503–1521. doi: 10.1785/0120120128

Weaver R., Pringle, P.T., 2003. Use of dendrochronology to date and better understand the Bonneville landslide, Columbia River Gorge, Washington, Geological Society of America Abstract with Programs 35.

Wells, R.E., Heller, P.L., 1988. The relative contribution of accretion, shear, and extension to Cenozoic tectonic rotation in the Pacific Northwest. Geological Society of America Bulletin 100, 325–338. doi: 10.1130/0016-7606(1988)

Wells, R.E., McCaffrey, R., 2013. Steady rotation of the Cascade arc. Geology 41, 1027–1030. doi: 10.1130/G34514.1

Wells, R.E., Weaver, C.S., Blakely, R.J., 1998. Fore-arc migration in Cascadia and its neotectonic significance. Geology 26, 759–762.

Yamaguchi, D.L., 1991. A simple method for cross-dating increment cores from living trees. Canadian Journal of Forest Research 21, 414-416. doi: 10.1139/x91-053.

Yamaguchi, D.K., Atwater, B.F., Bunker, D.E., Benson, B.E., Reid, M.S., 1997. Tree-ring dating the 1700 Cascadia earthquake. Nature 389, 922–923.

PROJECT DATA:

The data will be made publicly available through the University of Arizona Dendro database and the samples will be permanently archived at the Laboratory of Tree-Ring Research (LTRR) using established protocols. Radiocarbon results will be archived via http://www.geochron.org/

ADDITIONAL PRODUCTS:

Lahusen, S., A.R. Duvall, A.M. Booth, A. Grant, J. Wartman, W. Struble, J. Roering, and D. Montgomery, (2018), Megathrust Earthquakes and Coseismic Landslides in Cascadia: Insights from a New Inventory of Thousands of Landslides Dated Using Calibrated Surface Roughness, *AGU Fall Mtg, Washington, D.C.*

Tuesday, 11 December 2018 13:55 - 14:10 Walter E Washington Convention Center - 147A

ABSTRACT: Coseismic landslides are major secondary hazards of large earthquakes, often responsible for much of the total human and economic losses and significant alteration of the landscape. In the Pacific Northwest U.S., large earthquakes up to magnitude 9 have been shown to occur, on average, every ~300-600 years along the Cascadia Subduction Zone megathrust. The latest such event occurred 318 years before present, in AD 1700. Despite excellent constraints on the timing of this earthquake, the effects of intense shaking on the landscape are poorly understood. Regression models from historical coseismic landslide inventories predict thousands of landslides triggered by a magnitude 9 earthquake, but not a single landslide has yet been definitively linked to the AD 1700 quake. Here, we interrogate spatial and temporal patterns in landsliding in the central Oregon Coast Range (OCR) using a newly mapped inventory of 5,000 deep-seated landslides within Tyee Formation rocks. With this new dataset, we will apply a landslide surface roughness dating technique first trained on deep-seated slides near Oso, WA. This approach augments quantitative surface roughness analysis with a suite of radiocarbon and dendrochronology ages for 14 landslides ranging in age from 200 – 40,000 ybp, including 12 landslides not previously dated. Using roughness as a proxy for age, we develop an extensive regional landslide chronology covering 4,000 square km of the OCR and assess clustering in landslide timing and location (distance from the megathrust). Beyond looking for patterns in AD 1700 coseismic landslides, our inventory offers an unparalleled look at how landslides erode this tectonically active landscape on longer timescales, acting to limit orogenic growth over hundreds of earthquake cycles.

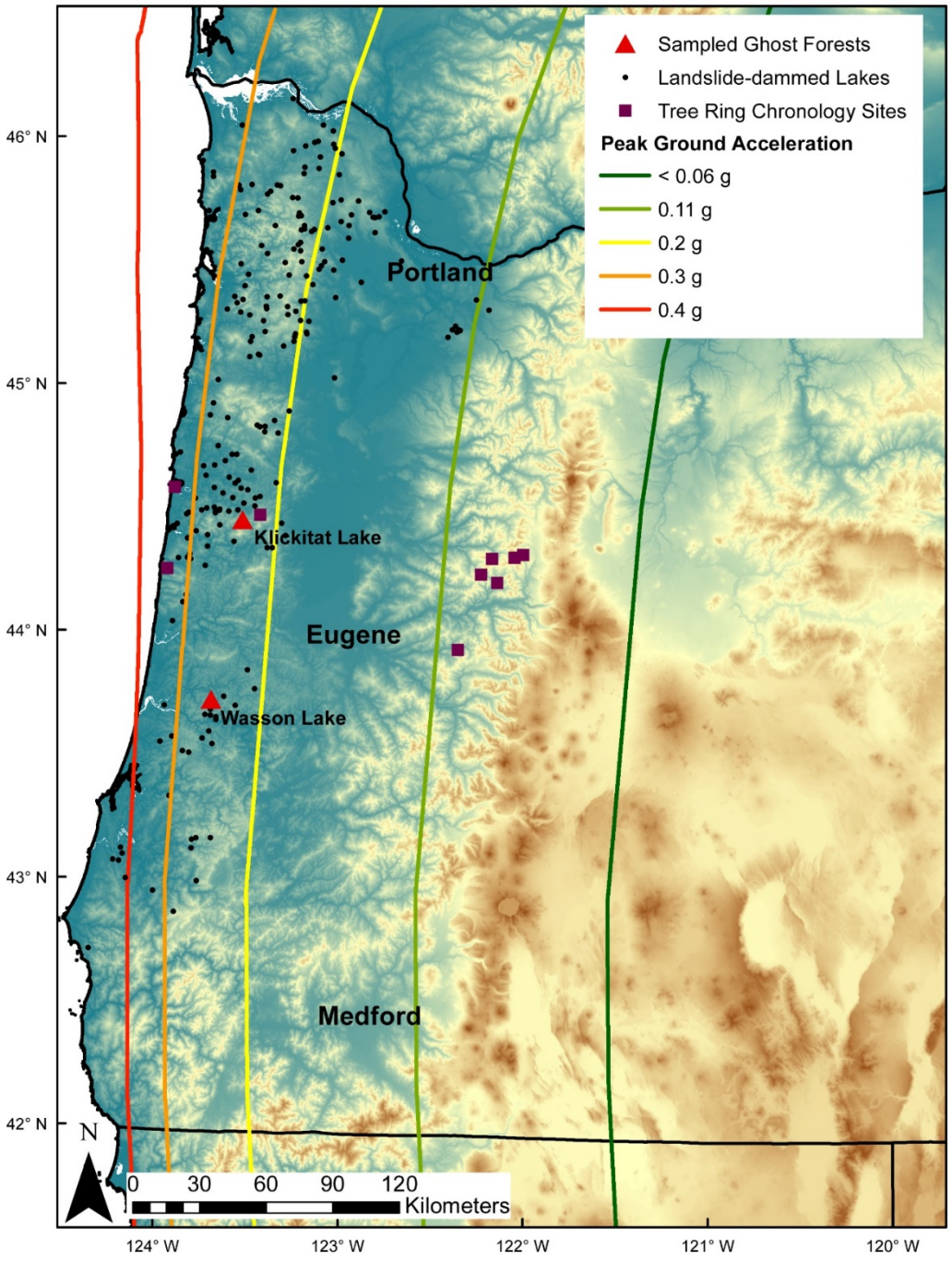

Figure 1: Western Oregon and landslide-dammed lakes. Red triangles represent the two landslide-dammed lakes we date in this study, Wasson Lake and Klickitat Lake. Maroon squares are the sites of Douglas-fir chronologies constructed in Black et al. (2015). Scaled color contours represent the expected peak ground acceleration during a M_w 9 Cascadia subduction zone earthquake (Madin and Burns, 2013).

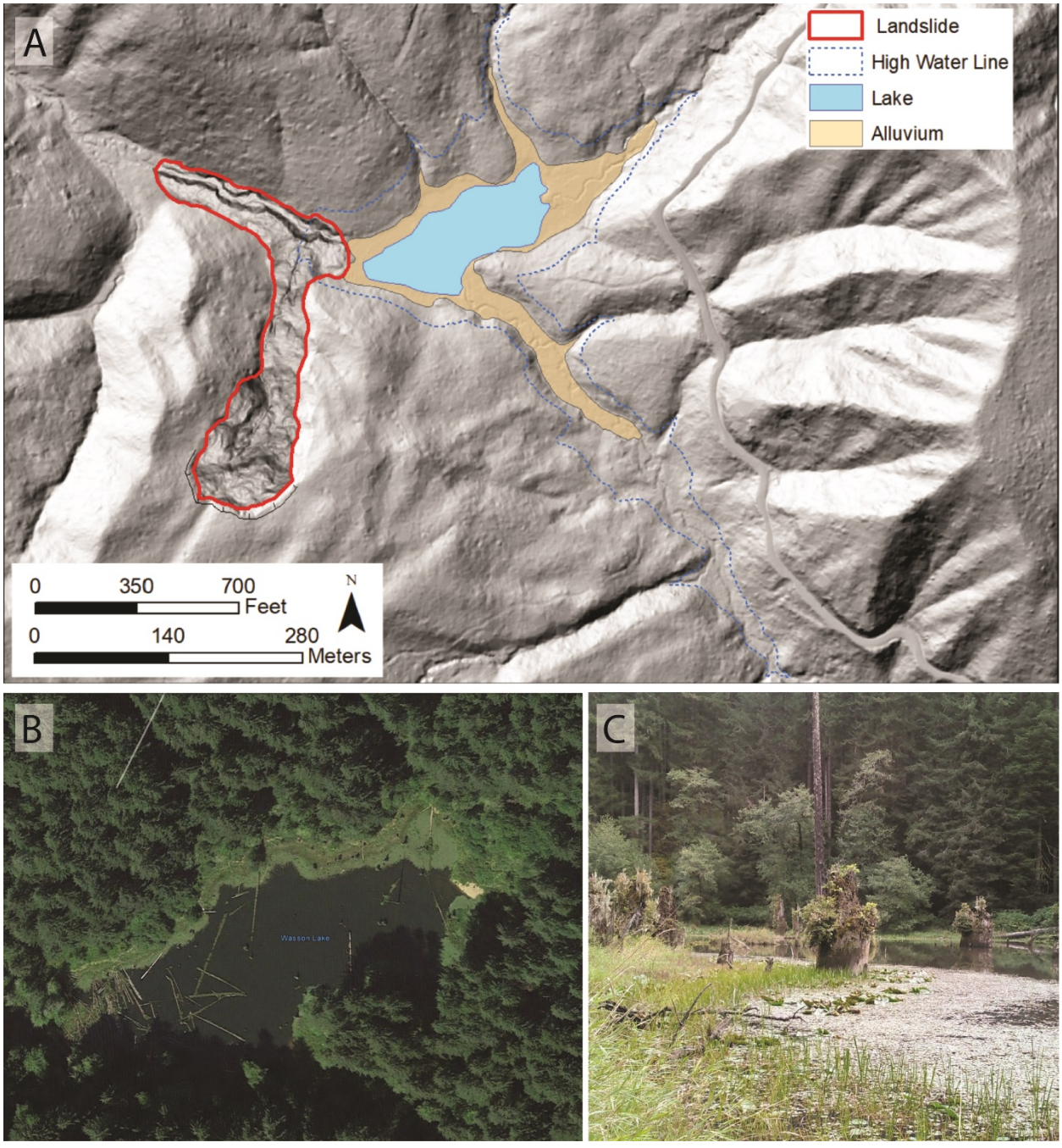

Figure 2: **A.** Map of the Wasson Lake site, including the current and estimated high water levels, with the landslide dam outlined in red. **B.** Aerial imagery of Wasson Lake. **C.** Standing Douglas-fir snags in Wasson Lake.

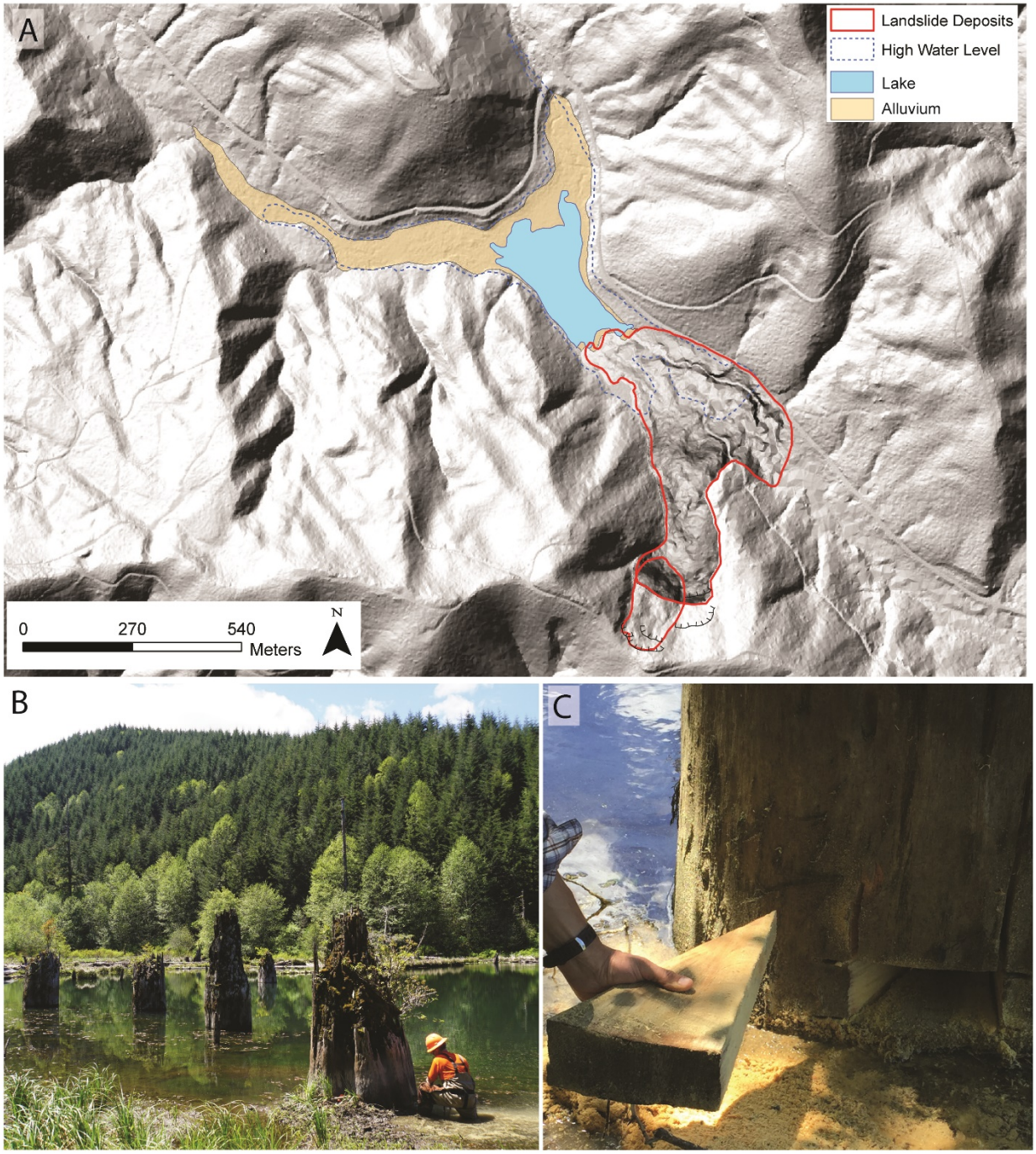

Figure 3: **A.** Map of the Klickitat Lake site, including the current and estimated high water levels, with the landslide dam outlined in red. **B.** Sampling Douglas-fir snags in Klickitat Lake. **C.** Example of slab extracted from standing snag.

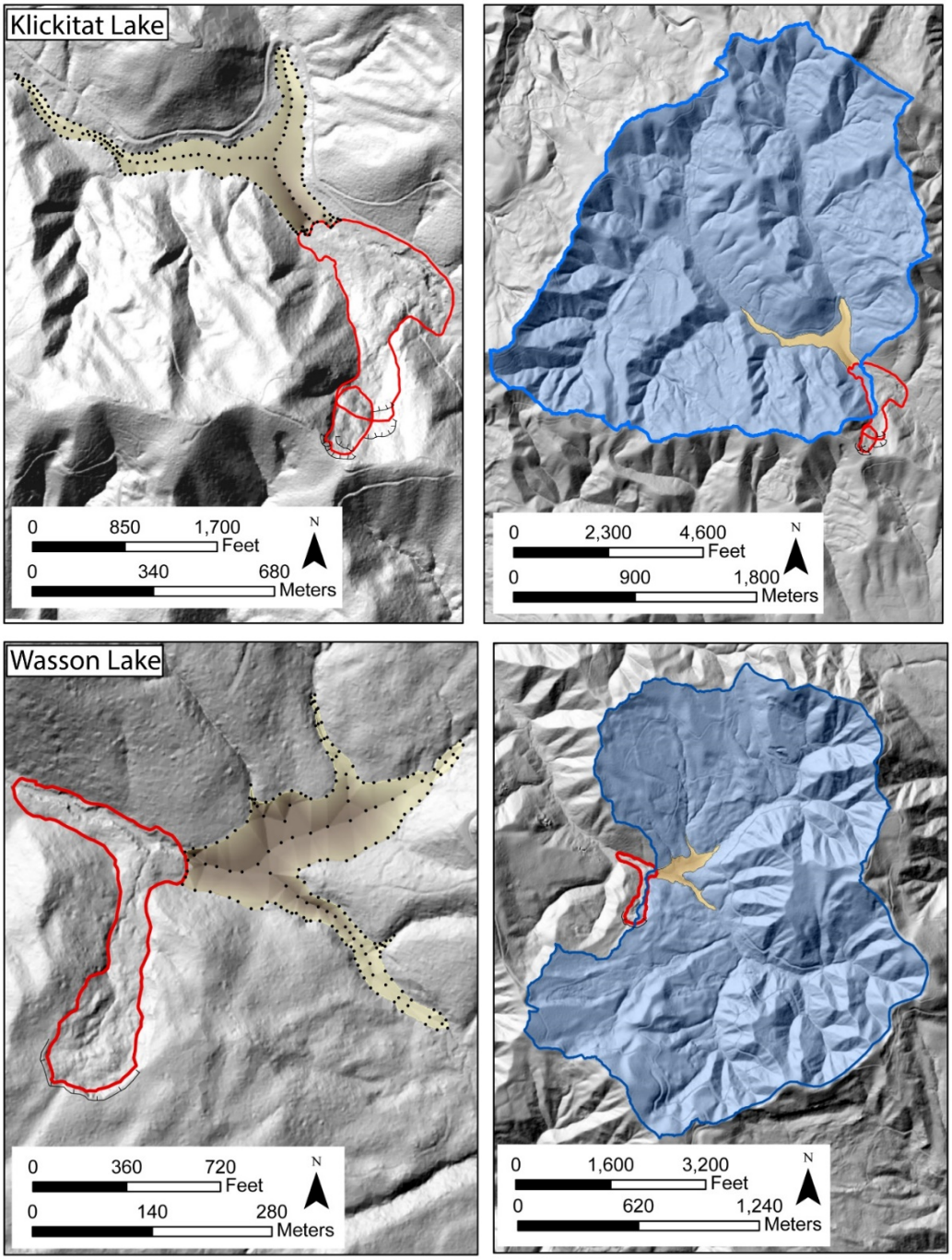

Figure 4: Maps of the estimated pre-sediment infill DEM (brown) and elevation points (black dots) used to calculate landslide age from valley alluviation at Klickitat and Wasson Lakes. Watershed extent above landslide dam highlighted in blue.

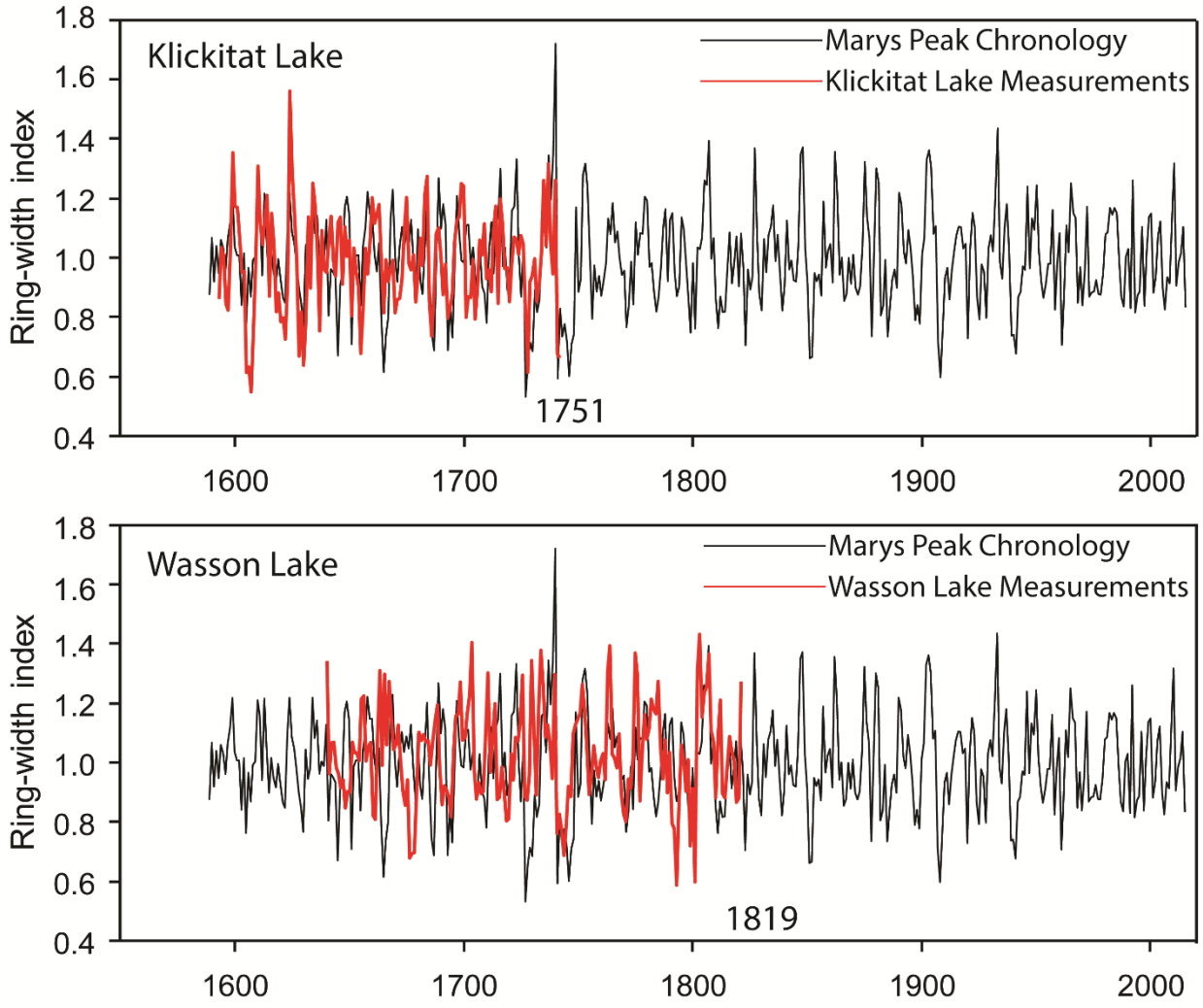

Figure 5: Examples of the measurement time-series for Klickitat and Wasson Lakes lagged and fit against the Marys Peak Chronology. The lagged correlation coefficient corresponding to these two dates is conspicuously high relative to other potential years, thus showing the year of death of the trees and accurate dating of the landslide.

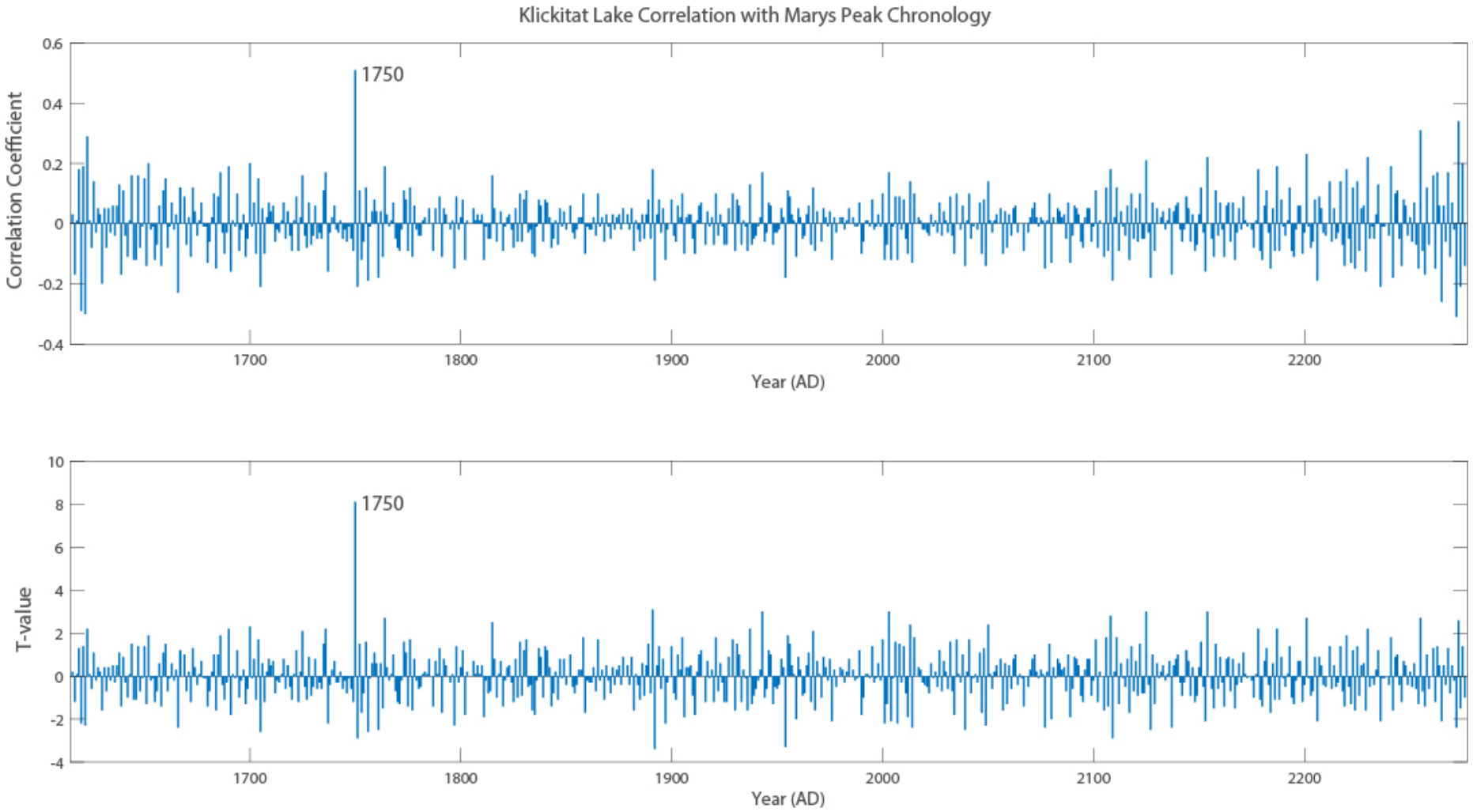

Figure 6: Correlation plots for hanging chronology generated at Klickitat Lake lagged against chronology from Marys Peak, Oregon (Black et al., 2015). Both the correlation coefficient and T-value (correlation coefficient normalized by the sample size) are significantly and conspicuously high for the year 1750, relative to other years. Note that the year 1750 corresponds to the last *measured* ring, while 1751 was the year of the last growth increment.

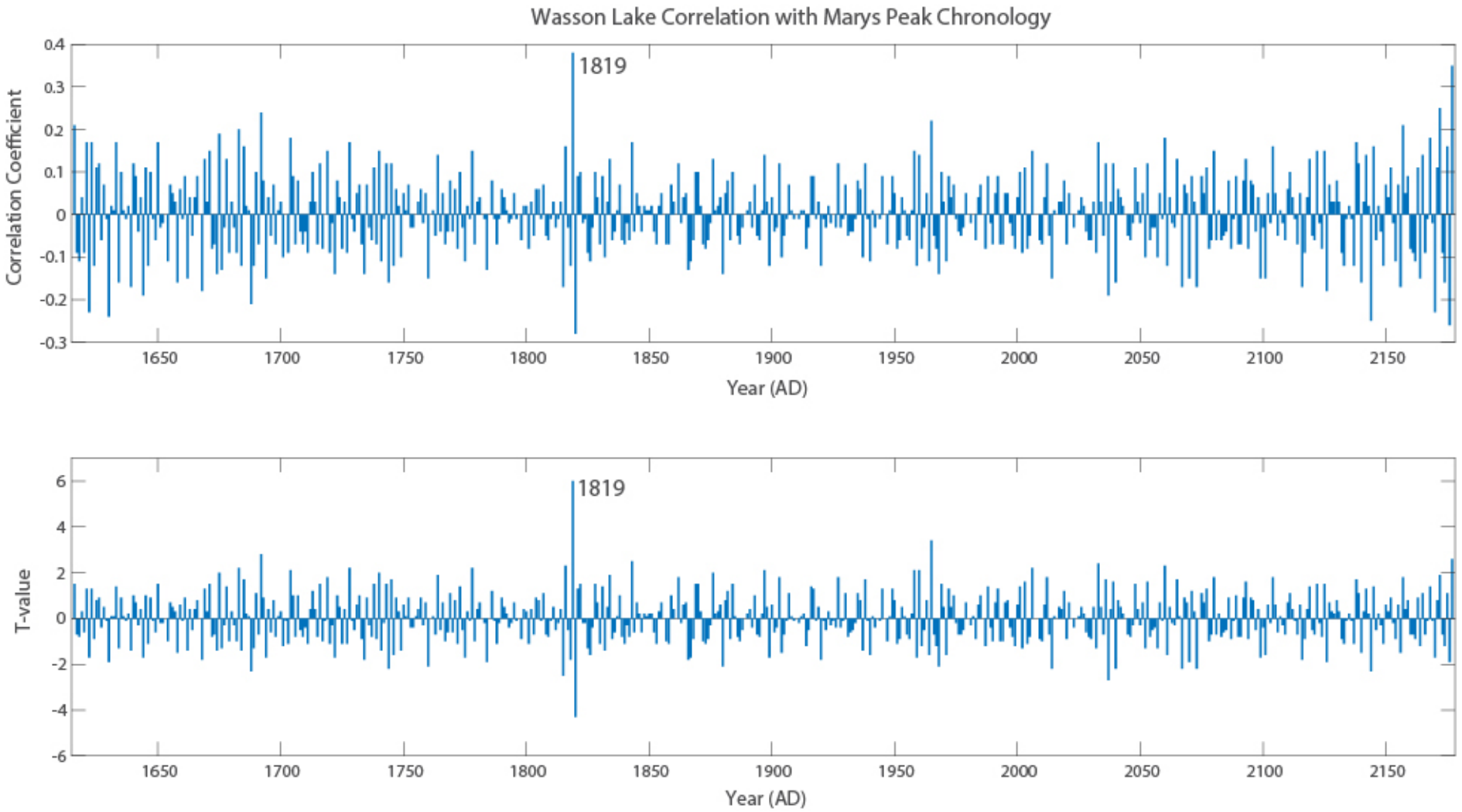

Figure 7: Correlation plots for hanging chronology generated at Wasson Lake lagged against chronology from Marys Peak, Oregon (Black et al., 2015). Both the correlation coefficient and T-value (correlation coefficient normalized by the sample size) are significantly and conspicuously high for the year 1819, relative to other years.

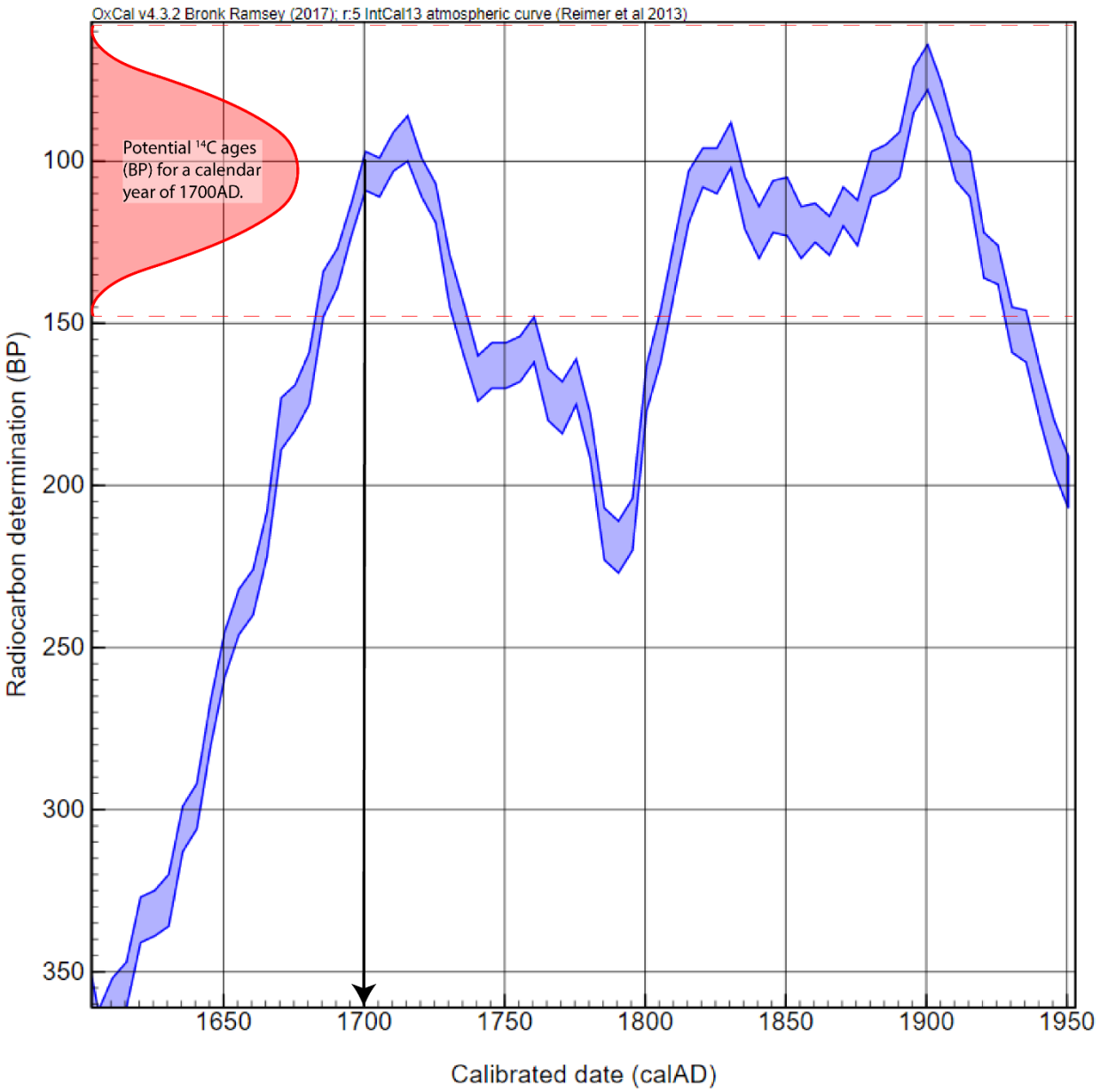

Figure 8: Radiocarbon calibration curve (blue) between 1600 AD and present (1950). Note the oscillation of the curve, resulting in several potential calendar year (Calibrated date) ages for each ^{14}C sample (Radiocarbon determination). If searching for a specific event, such as the 1700 AD earthquake, multiple values ^{14}C ages could suggest, possibly erroneously, a calendar year of 1700 AD. Red PDF provides range of potential ^{14}C ages that may suggest 1700 AD as a possible calendar year age. Figure modified from Reimer et al. (2013).

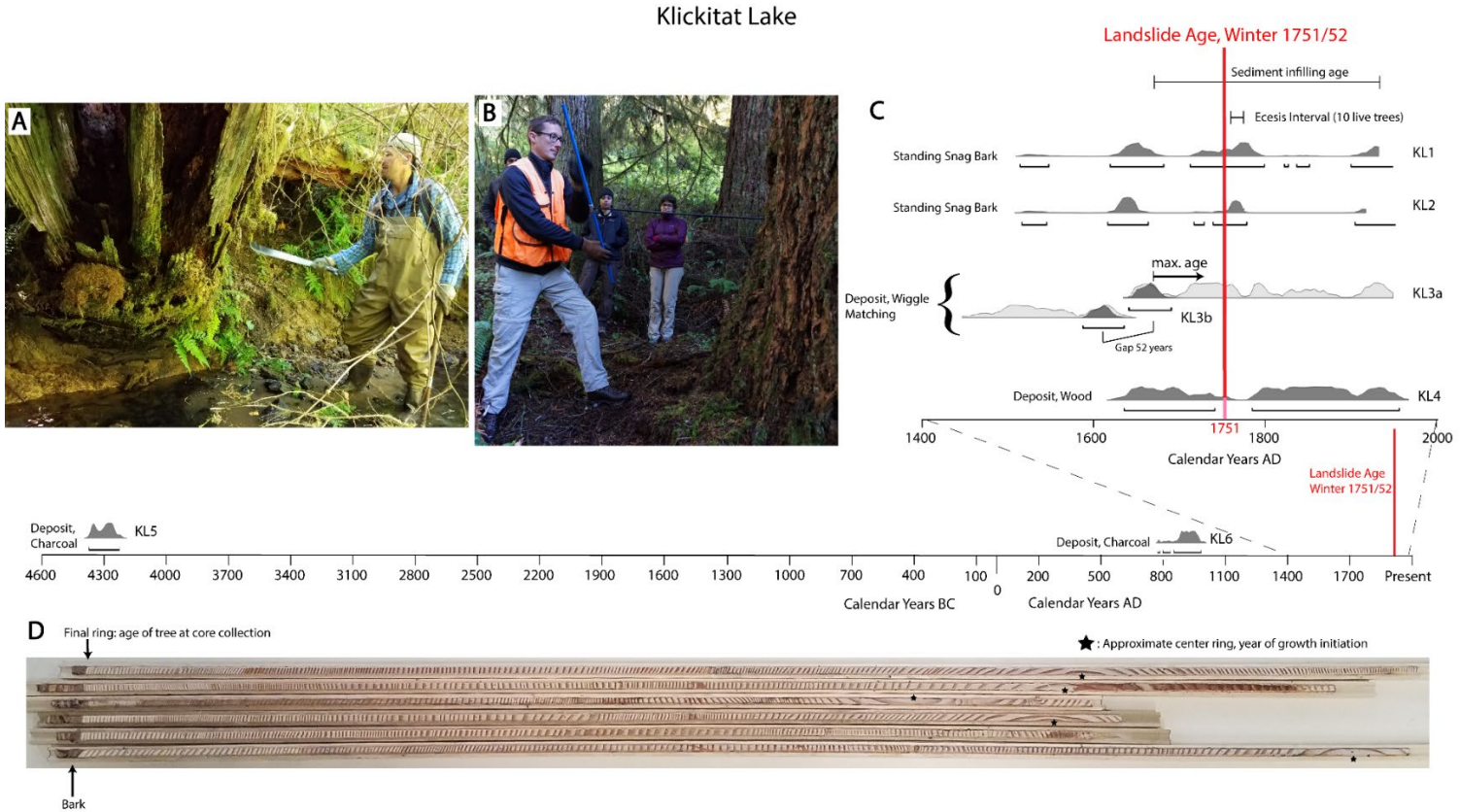

Figure 9: **A.** Example of large log buried by landslide deposit. Samples from this tree were collected from the outermost exposed wood. **B.** Collection of live cores from live old growth on the landslide deposit. **C.** Radiocarbon results from Klickitat Lake. Each sample labeled according to the type of material (wood, bark, charcoal) and its relative location (lake, deposit). Each sample age is displayed as a PDF, based on where its ^{14}C age lies relative to the ^{14}C calibration curve. Multiple PDFs for a single sample represent a part of the radiocarbon calibration curve that has multiple 'wiggles.' Sample KL3 is a wiggle matched sample, where wood from two rings separated by 52 rings produces two separate PDFs, which are then constrained given the inner ring must be 52 years older than the outer ring. The sediment infilling ages are calculated from alluviated portions of the landslide-dammed lake and valley and span over a range of potential erosion rates. Absolute landslide age from dendrochronology represented as a red line in the winter of 1751-52. **D.** Example of cores collected from live old growth on the landslide surface, as seen in **B.**. These trees cannot be older than the dendrochronology-derived age. The cores from these trees show that they began growing approximately a decade after landslide emplacement, labeled the ecesis interval in **C.**

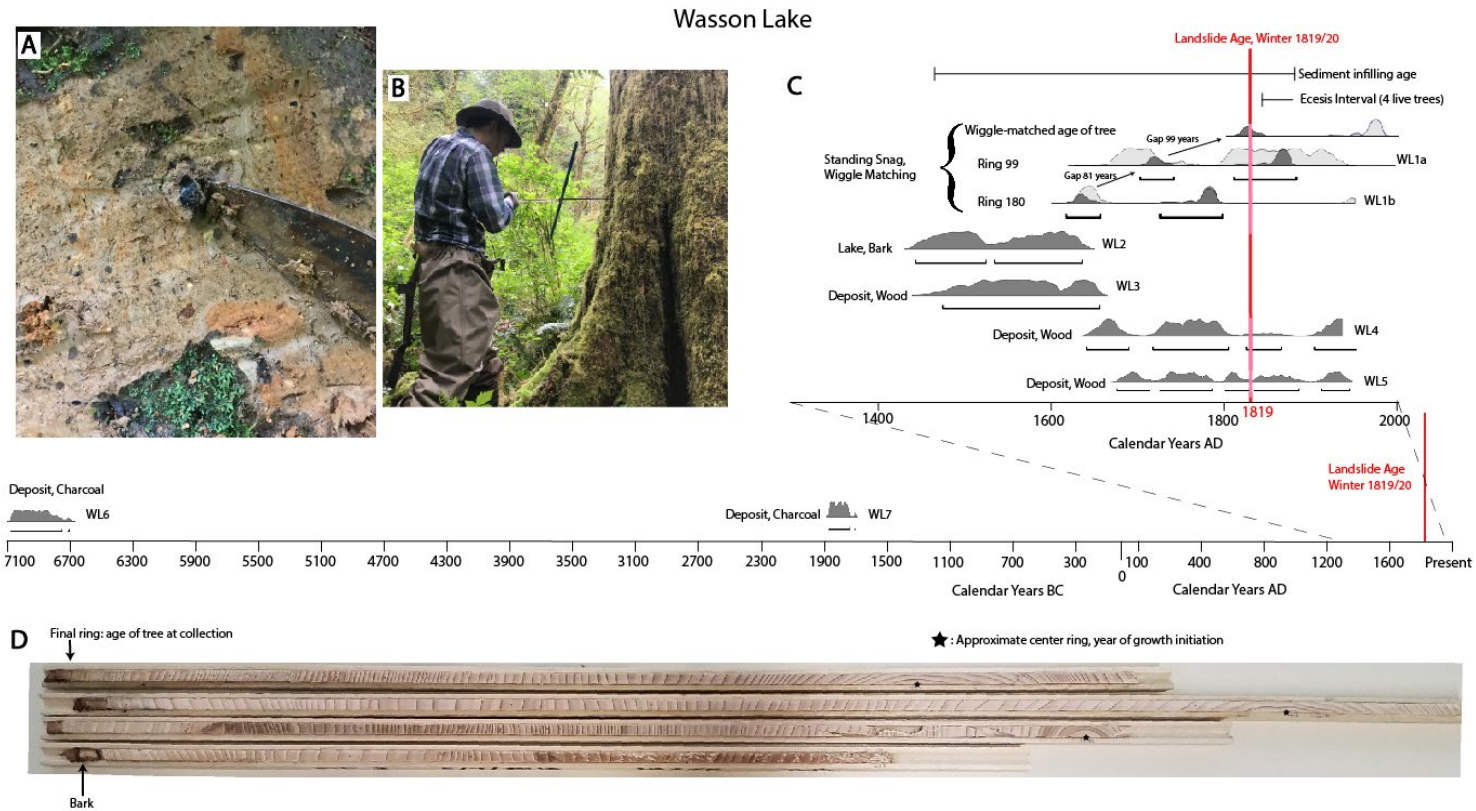

Figure 10: **A.** Charcoal buried in the landslide deposit at Wasson Lake. **B.** Collection of live cores from live old growth on the landslide deposit. **C.** Radiocarbon results from Wasson Lake. Each sample labeled according to the type of material (wood, bark, charcoal) and its relative location (lake, deposit). Each sample age is displayed as a PDF, based on where its ^{14}C age lies relative to the ^{14}C calibration curve. Multiple PDFs for a single sample represent a part of the radiocarbon calibration curve that has multiple 'wiggles.' Wiggle matched sample constrains the time of death PDF by using the 81-year gap between the inner ring and outer ring to require the inner ring to be the older sample, and then counting out the final 99 years to the year the tree died. The sediment infilling ages are calculated from alluviated portions of the landslide-dammed lake and valley and span over a range of potential erosion rates. Absolute landslide age from dendrochronology represented as a red line in the winter of 1819/20. **D.** Example of cores collected from live old growth on the landslide surface, as seen in **B.** These trees cannot be older than the dendrochronology-derived age. The cores from these trees show that they began growing approximately a decade after landslide emplacement, labeled the ecesis interval in **C**